Humanoid robots - Differential kinematics and statics

Mgr. Matěj Hoffmann, Ph.D.

Geometrical Jacobian

$$\nu = \overset{\text{twist}}{\begin{bmatrix} v \\ \omega \end{bmatrix}} = \begin{bmatrix} \dot{x} \\ \dot{y} \\ \dot{z} \\ \omega_x \\ \omega_y \\ \omega_z \end{bmatrix} = \begin{bmatrix} \frac{\partial x}{\partial q_1} & \frac{\partial x}{\partial q_2} & \cdots & \frac{\partial x}{\partial q_n} \\ \frac{\partial y}{\partial q_1} & \frac{\partial y}{\partial q_2} & \cdots & \frac{\partial y}{\partial q_n} \\ \vdots & \vdots & \vdots & \vdots \\ \frac{\partial \omega_z}{\partial q_1} & \frac{\partial \omega_z}{\partial q_2} & \cdots & \frac{\partial \omega_z}{\partial q_n} \end{bmatrix} \begin{bmatrix} \dot{q}_1 \\ \vdots \\ \dot{q}_n \end{bmatrix} = J(q) \cdot \dot{q}$$

- it is a function of the joint configuration q
- contains all of the partial derivatives of f , relating every joint angle to every velocity
- tells us how small changes in joint space will affect the end-effector's position in Cartesian space
- columns: how each component of velocity changes when the configuration (i.e., angle) of a particular joint changes
- rows: how movement in each joint affects a particular component of velocity

3.3.1 in Nikolaus Correll, Bradley Hayes, Christoffer Heckman and Alessandro Roncone. Introduction to Autonomous Robots: Mechanisms, Sensors, Actuators, and Algorithms, MIT Press, 2022 (forthcoming). https://github.com/Introduction-to-Autonomous-Robots/Introduction-to-Autonomous-Robots

Analytical Jacobian

$$\mathbf{x} = \mathbf{f}(\mathbf{q}) \overset{d/dt}{\Longrightarrow} \dot{\mathbf{x}} = \mathbf{J}(\mathbf{q})\dot{\mathbf{q}}$$

$$\mathbf{J}(\mathbf{q}) = \begin{bmatrix} \frac{\partial f_1}{\partial q_1} & \cdots & \frac{\partial f_1}{\partial q_n} \\ \vdots & \ddots & \vdots \\ \frac{\partial f_m}{\partial q_1} & \cdots & \frac{\partial f_m}{\partial q_n} \end{bmatrix}$$

$$\dot{\mathbf{x}} = \begin{bmatrix} \dot{\mathbf{p}} \\ \dot{\phi} \end{bmatrix} = \begin{bmatrix} \mathbf{J}_P \\ \mathbf{J}_\phi \end{bmatrix} \dot{\mathbf{q}}$$

Slide source: https://github.com/vvv-school/vvv18/blob/master/material/kinematics/kinematics.pdf. Courtesy Ugo Pattacini.

Planar arm with 2 rotational joints - forward kinematics (position only)

$$
\begin{aligned}
x_1 &= L_1 \cos\theta_1 + L_2 \cos(\theta_1 + \theta_2) \\
x_2 &= L_1 \sin\theta_1 + L_2 \sin(\theta_1 + \theta_2).
\end{aligned}
$$

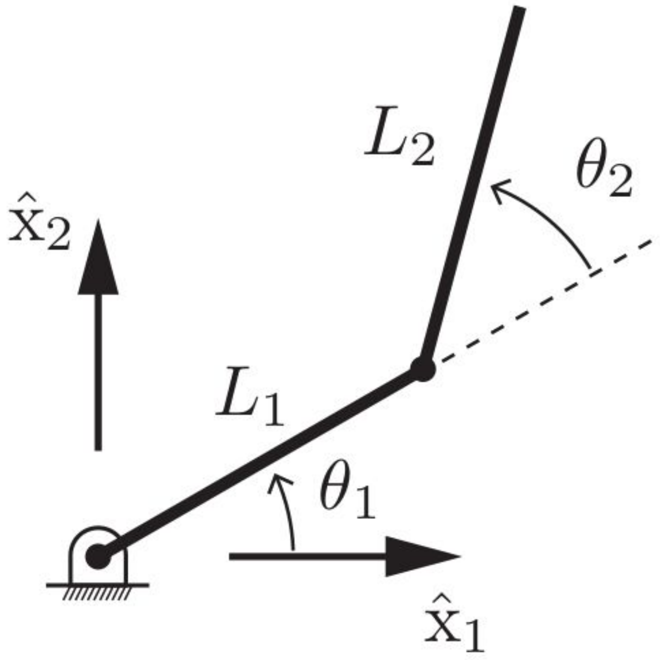

Ch.5 Velocity kinematics and statics in Lynch, K. M., & Park, F. C. (2017). Modern robotics. Cambridge University Press.
(see also https://youtu.be/6tj8QLF69Ok)

Planar arm with 2 rotational joints - forward differential kinematics (position only)

$$x_1 = L_1 \cos\theta_1 + L_2 \cos(\theta_1+\theta_2)$$
$$x_2 = L_1 \sin\theta_1 + L_2 \sin(\theta_1+\theta_2).$$

Differentiating both sides with respect to time yields

$$\dot{x}_1 = -L_1\dot{\theta}_1 \sin\theta_1 - L_2(\dot{\theta}_1+\dot{\theta}_2)\sin(\theta_1+\theta_2)$$
$$\dot{x}_2 = L_1\dot{\theta}_1 \cos\theta_1 + L_2(\dot{\theta}_1+\dot{\theta}_2)\cos(\theta_1+\theta_2),$$

which can be rearranged into an equation of the form $\dot{x} = J(\theta)\dot{\theta}$:

$$\begin{bmatrix} \dot{x}_1 \\ \dot{x}_2 \end{bmatrix} = \begin{bmatrix} -L_1\sin\theta_1 - L_2\sin(\theta_1+\theta_2) & -L_2\sin(\theta_1+\theta_2) \\ L_1\cos\theta_1 + L_2\cos(\theta_1+\theta_2) & L_2\cos(\theta_1+\theta_2) \end{bmatrix} \begin{bmatrix} \dot{\theta}_1 \\ \dot{\theta}_2 \end{bmatrix}. \quad (5.1)$$

Writing the two columns of $J(\theta)$ as $J_1(\theta)$ and $J_2(\theta)$, and the tip velocity $\dot{x}$ as v_{tip}, Equation (5.1) becomes

$$v_{\text{tip}} = J_1(\theta)\dot{\theta}_1 + J_2(\theta)\dot{\theta}_2. \quad (5.2)$$

$J_1(\theta) + J_2(\theta)$: basis for the linear velocities of the end effector (with coefficients equal to joint velocities)

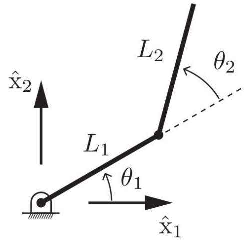

end effector velocity when joint 1 rotates at unit speed (joint 2 is still)

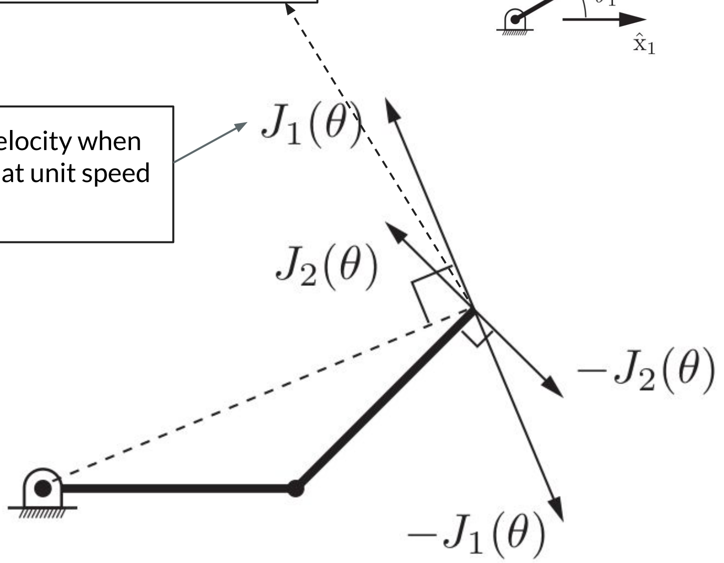

Ch.5 Velocity kinematics and statics in Lynch, K. M., & Park, F. C. (2017). Modern robotics. Cambridge University Press. (see also https://youtu.be/6tj8QLF69Ok)

Straightforward generalization to 3D

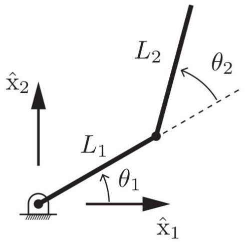

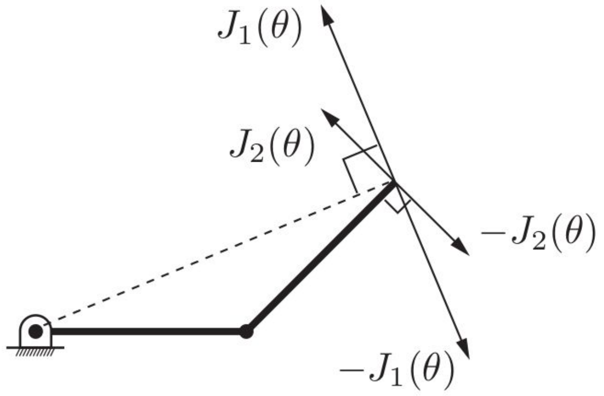

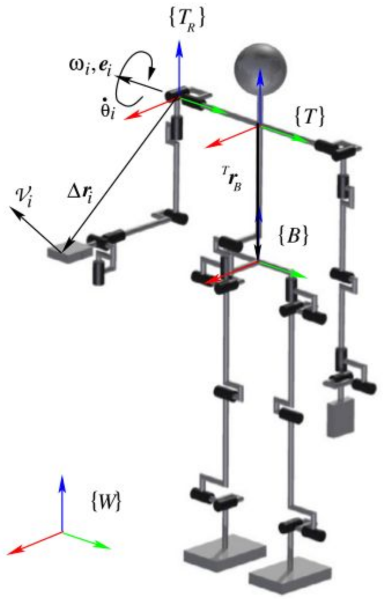

FIGURE 2.3 End-link spatial velocity $\mathcal{J}_i = [(e_i \times r_i)^T \;\; e_i^T]^T$ is obtained with joint rate $\dot{\theta}_i = 1$ rad/s. Vector e_i signifies the joint axis of rotation. The position r_i of the characteristic point on the end link is determined w.r.t. reference frame $\{T_R\}$, obtained by translating the common root frame for the arms, $\{T\}$, to a suitably chosen point on the joint axis, e.g. according to the Denavit and Hartenberg notation [26].

Section 2.4 in Nenchev, D. N., Konno, A., & Tsujita, T. (2018). Humanoid robots: Modeling and control. Butterworth-Heinemann.

Planar arm with 2 rotational joints - singularities (position only)

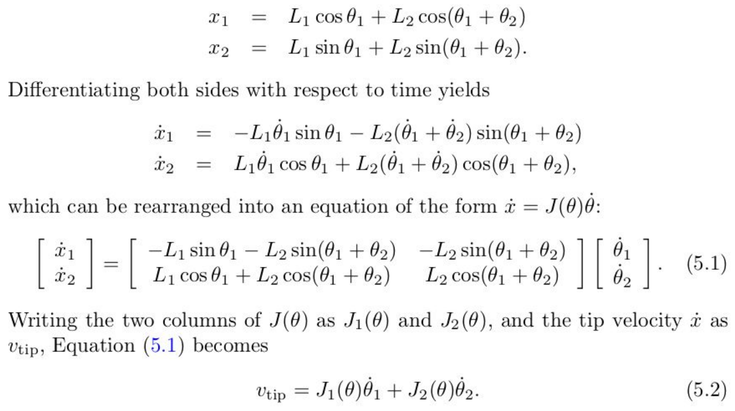

$$\begin{aligned} x_1 &= L_1 \cos\theta_1 + L_2 \cos(\theta_1+\theta_2) \\ x_2 &= L_1 \sin\theta_1 + L_2 \sin(\theta_1+\theta_2). \end{aligned}$$

Differentiating both sides with respect to time yields

$$\begin{aligned} \dot{x}_1 &= -L_1\dot{\theta}_1 \sin\theta_1 - L_2(\dot{\theta}_1+\dot{\theta}_2)\sin(\theta_1+\theta_2) \\ \dot{x}_2 &= L_1\dot{\theta}_1 \cos\theta_1 + L_2(\dot{\theta}_1+\dot{\theta}_2)\cos(\theta_1+\theta_2), \end{aligned}$$

which can be rearranged into an equation of the form $\dot{x} = J(\theta)\dot{\theta}$:

$$\begin{bmatrix} \dot{x}_1 \\ \dot{x}_2 \end{bmatrix} = \begin{bmatrix} -L_1\sin\theta_1 - L_2\sin(\theta_1+\theta_2) & -L_2\sin(\theta_1+\theta_2) \\ L_1\cos\theta_1 + L_2\cos(\theta_1+\theta_2) & L_2\cos(\theta_1+\theta_2) \end{bmatrix} \begin{bmatrix} \dot{\theta}_1 \\ \dot{\theta}_2 \end{bmatrix}. \quad (5.1)$$

Writing the two columns of $J(\theta)$ as $J_1(\theta)$ and $J_2(\theta)$, and the tip velocity $\dot{x}$ as v_{tip}, Equation (5.1) becomes

$$v_{\text{tip}} = J_1(\theta)\dot{\theta}_1 + J_2(\theta)\dot{\theta}_2. \quad (5.2)$$

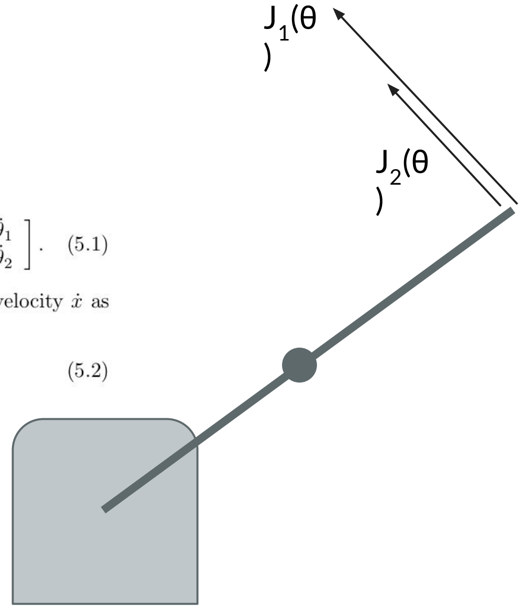

- θ_2 = 0° (or 180°)
- $J_1(\theta)$ and $J_2(\theta)$ aligned
- impossible to generate any end effector velocity except along this line
- dimension of the column space of the Jacobian drops from its maximum value

Ch.5 Velocity kinematics and statics in Lynch, K. M., & Park, F. C. (2017). Modern robotics. Cambridge University Press. (see also https://youtu.be/6tj8QLF69Ok)

Manipulability ellipsoid

- Unit circle of joint velocities maps through the Jacobian to an ellipse in the space of tip velocities - the *manipulability ellipsoid.*
- As the manipulator configuration approaches a singularity, the ellipse collapses to a line segment, since the ability of the tip to move in one direction is lost.

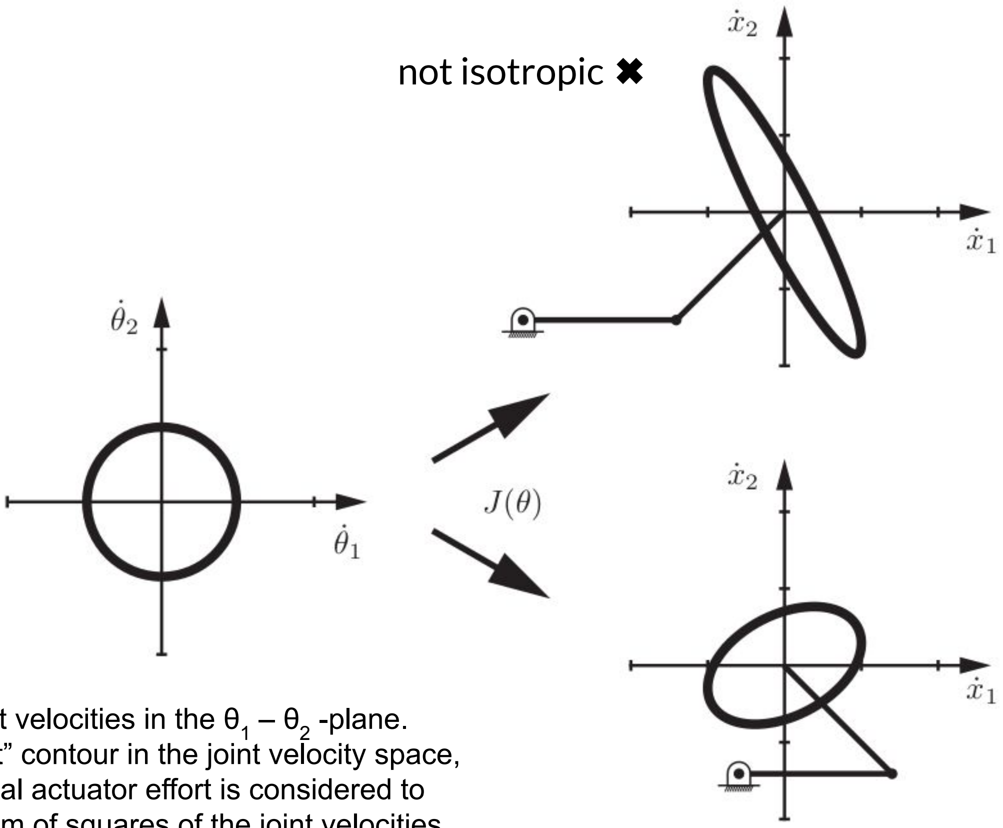

Unit circle of joint velocities in the $\theta_1 - \theta_2$ -plane.

- “iso-effort” contour in the joint velocity space, where total actuator effort is considered to be the sum of squares of the joint velocities

Ch.5 Velocity kinematics and statics in Lynch, K. M., & Park, F. C. (2017). Modern robotics. Cambridge University Press. (see also https://youtu.be/6tj8QLF69Ok)

Manipulability

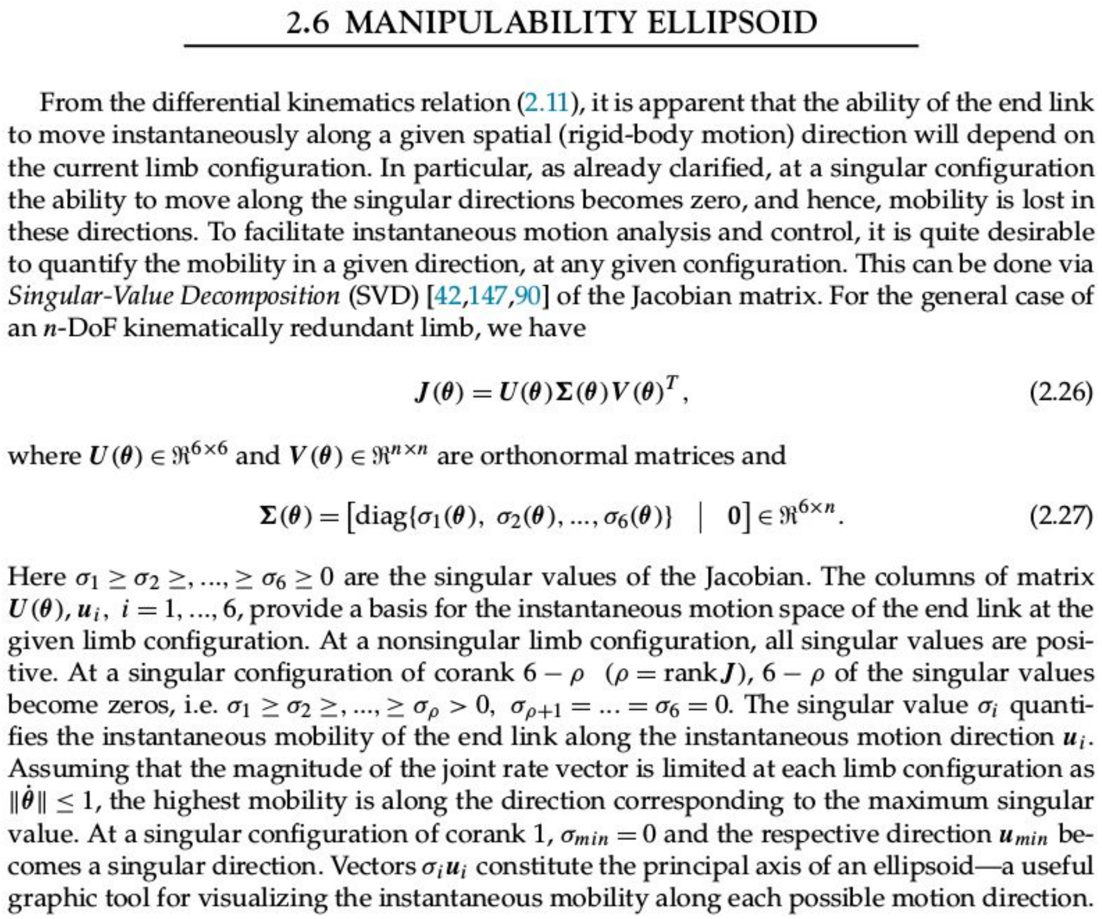

2.6 MANIPULABILITY ELLIPSOID

From the differential kinematics relation (2.11), it is apparent that the ability of the end link to move instantaneously along a given spatial (rigid-body motion) direction will depend on the current limb configuration. In particular, as already clarified, at a singular configuration the ability to move along the singular directions becomes zero, and hence, mobility is lost in these directions. To facilitate instantaneous motion analysis and control, it is quite desirable to quantify the mobility in a given direction, at any given configuration. This can be done via *Singular-Value Decomposition* (SVD) [42,147,90] of the Jacobian matrix. For the general case of an n-DoF kinematically redundant limb, we have

$$\boldsymbol{J}(\boldsymbol{\theta}) = \boldsymbol{U}(\boldsymbol{\theta})\boldsymbol{\Sigma}(\boldsymbol{\theta})\boldsymbol{V}(\boldsymbol{\theta})^T, \tag{2.26}$$

where $\boldsymbol{U}(\boldsymbol{\theta}) \in \Re^{6\times 6}$ and $\boldsymbol{V}(\boldsymbol{\theta}) \in \Re^{n\times n}$ are orthonormal matrices and

$$\boldsymbol{\Sigma}(\boldsymbol{\theta}) = \left[\operatorname{diag}\{\sigma_1(\boldsymbol{\theta}),\ \sigma_2(\boldsymbol{\theta}), ..., \sigma_6(\boldsymbol{\theta})\} \quad \middle| \quad \boldsymbol{0}\right] \in \Re^{6\times n}. \tag{2.27}$$

Here $\sigma_1 \geq \sigma_2 \geq, ..., \geq \sigma_6 \geq 0$ are the singular values of the Jacobian. The columns of matrix $\boldsymbol{U}(\boldsymbol{\theta})$, $\boldsymbol{u}_i,\ i = 1, ..., 6$, provide a basis for the instantaneous motion space of the end link at the given limb configuration. At a nonsingular limb configuration, all singular values are positive. At a singular configuration of corank $6-\rho \quad (\rho = \operatorname{rank}\boldsymbol{J})$, $6-\rho$ of the singular values become zeros, i.e. $\sigma_1 \geq \sigma_2 \geq, ..., \geq \sigma_\rho > 0,\ \ \sigma_{\rho+1} = ... = \sigma_6 = 0$. The singular value σ_i quantifies the instantaneous mobility of the end link along the instantaneous motion direction $\boldsymbol{u}_i$. Assuming that the magnitude of the joint rate vector is limited at each limb configuration as $\|\dot{\boldsymbol{\theta}}\| \leq 1$, the highest mobility is along the direction corresponding to the maximum singular value. At a singular configuration of corank 1, $\sigma_{min} = 0$ and the respective direction $\boldsymbol{u}_{min}$ becomes a singular direction. Vectors $\sigma_i \boldsymbol{u}_i$ constitute the principal axis of an ellipsoid—a useful graphic tool for visualizing the instantaneous mobility along each possible motion direction.

Section 2.6 in Nenchev, D. N., Konno, A., & Tsujita, T. (2018). Humanoid robots: Modeling and control. Butterworth-Heinemann.

Manipulability ellipsoid

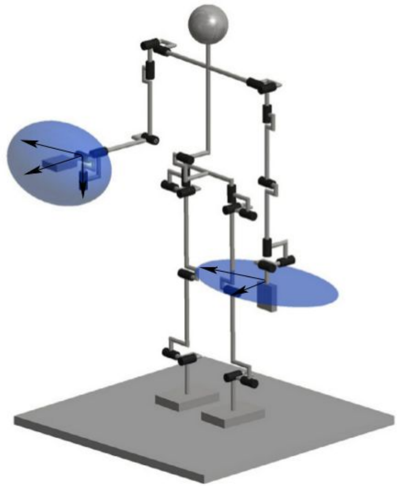

FIGURE 2.8 Manipulability ellipsoid for translational motion. The right arm is in a nonsingular configuration and the respective ellipsoid is 3D, with principal axes $\sigma_1 \boldsymbol{u}_1, \sigma_2 \boldsymbol{u}_2$, and $\sigma_3 \boldsymbol{u}_3$. The left arm is at a singular configuration: the downward translational mobility has been lost, and therefore, the manipulability ellipsoid is only 2D. The principal axes are $\sigma_1 \boldsymbol{u}_1$ and $\sigma_2 \boldsymbol{u}_2$.

The dimension of the ellipsoid is determined by the rank of the Jacobian. Fig. 2.8 shows a robot configuration wherein the right arm is at a nonsingular configuration, whereas the left one is at the elbow singularity. The two ellipsoids at the end links visualize the instantaneous translational motion abilities. The ellipsoid for the right arm is 3D (full translational mobility), while that for the left arm is flat (an ellipse). The ellipse lies in a plane parallel to the floor since translational mobility in the vertical direction is nil at the singularity. The ellipsoid-based instantaneous mobility analysis has been introduced in [166]; the ellipsoid is referred to as the *manipulability ellipsoid*.

Section 2.6 in Nenchev, D. N., Konno, A., & Tsujita, T. (2018). Humanoid robots: Modeling and control. Butterworth-Heinemann.

iCub matlab demo

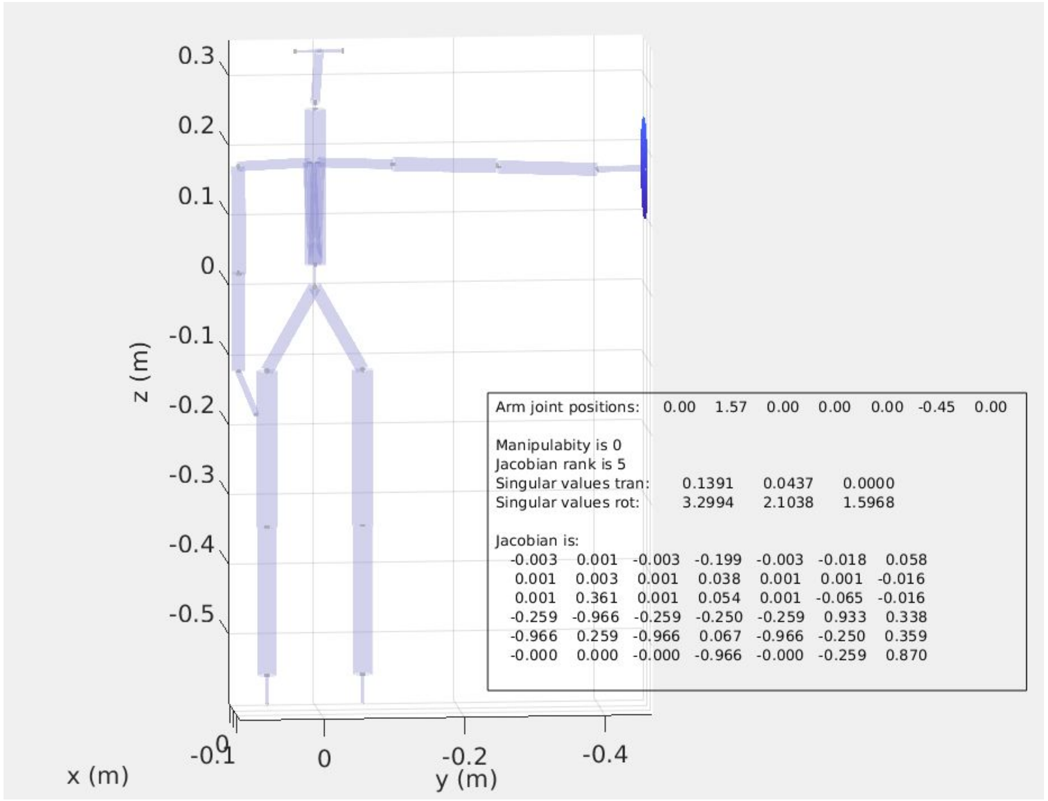

```
Arm joint positions:   0.00   1.57   0.00   0.00   0.00  -0.45   0.00

Manipulabity is 0
Jacobian rank is 5
Singular values tran:    0.1391    0.0437    0.0000
Singular values rot:     3.2994    2.1038    1.5968

Jacobian is:
  -0.003   0.001  -0.003  -0.199  -0.003  -0.018   0.058
   0.001   0.003   0.001   0.038   0.001   0.001  -0.016
   0.001   0.361   0.001   0.054   0.001  -0.065  -0.016
  -0.259  -0.966  -0.259  -0.250  -0.259   0.933   0.338
  -0.966   0.259  -0.966   0.067  -0.966  -0.250   0.359
  -0.000   0.000  -0.000  -0.966  -0.000  -0.259   0.870
```

See also:

- Vahrenkamp, N., Asfour, T., Metta, G., Sandini, G., & Dillmann, R. (2012, November). Manipulability analysis. In *2012 12th IEEE-RAS International Conference on Humanoid Robots (Humanoids 2012)* (pp. 568-573). IEEE.
- https://github.com/robotology/community/discussions/559#:~:text=Ipopt%20doesn%27t%20deal,Jacobian%20per%20se

The Jacobian and statics

The Jacobian can also be used to related forces and moments at the end effector to joint torques!

Terminology - kinematics, statics, dynamics, twists, wrenches...

- **Kinematics** - describes the motion of points, bodies (objects)... *without considering the forces* that cause them to move.
  - variables studied: position, velocity, acceleration (and their angular analogs)
  - ~ "geometry of motion"
  - *twist:* $\nu = \begin{bmatrix} v \\ \omega \end{bmatrix}$
- **Statics -** concerned with the analysis of (force and torque, or "moment") acting on physical systems that do not experience an acceleration (a=0), but rather, are in *static equilibrium* with their environment.
  - Wrench: F = $\begin{bmatrix} f \\ m \end{bmatrix}$ (or $\begin{bmatrix} f \\ \tau \end{bmatrix}$
- **Dynamics** (~ kinetics) - describes relationship between *motion* and its causes, specifically, forces and torques.
- All of the above are branches of classical mechanics.

Statics of open chains

- conservation of power:
  power at the joints = (power to move the robot) + (power at the end-effector)
- if the robot is in static equilibrium (no power used to move the robot):
  power at the joints = power at the end-effector
- Power (P)
  - W = F d; (W = F d cos θ) (displacement parallel to the force)
  - P = W/t = Fd / t = Fv; in rotational terms, P = τ ω
- Power at the joints = $\tau^T \dot{\theta}$
- Total P at the end effector = wrench · twist = $[F\ \tau]^T [v\ \omega] = \mathcal{F}^T \nu$

$\tau^T \dot{\theta} = \mathcal{F}^T \nu$ and $\nu = J(\theta)\dot{\theta}$

$\tau^T \dot{\theta} = \mathcal{F}^T J(\theta)\dot{\theta}$ and $(AB)^T = B^T A^T$

$$\tau = J(\theta)^T \mathcal{F}$$

- If external wrench - $\mathcal{F}$ is applied at the tip, we can obtain the joint torques opposing it - *force control.*

5.2 in Lynch, K. M., & Park, F. C. (2017). Modern robotics. Cambridge University Press / https://youtu.be/6tj8QLF69Ok?t=266

Velocity and force manipulability are orthogonal!

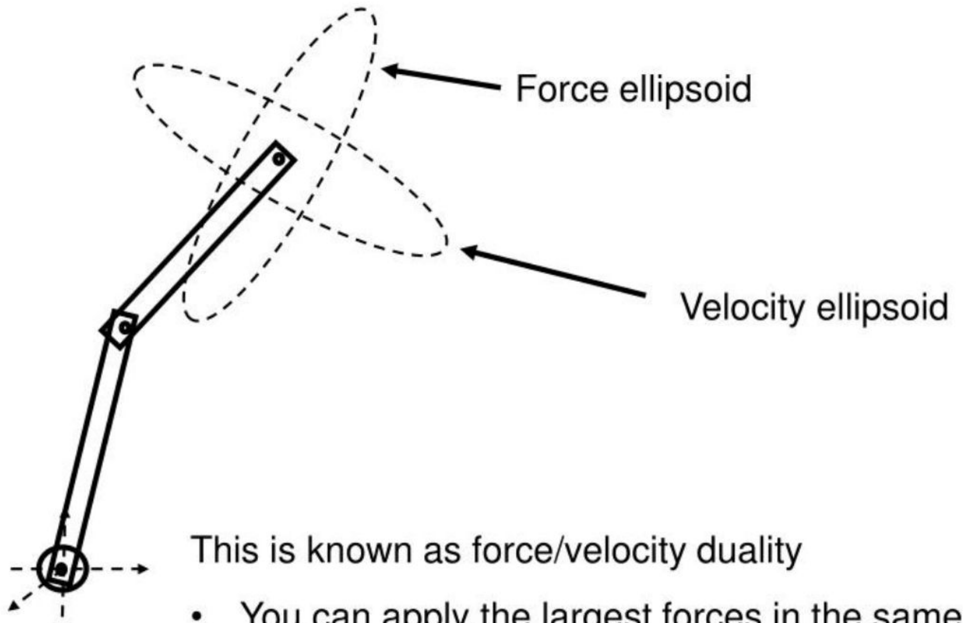

This is known as force/velocity duality

- You can apply the largest forces in the same directions that your max velocity is smallest
- Your max velocity is greatest in the directions where you can only apply the smallest forces

Slide 40 https://www.slideserve.com/antonia/inverting-the-jacobian-and-manipulability.
See slides 38-39 for details how this is derived.

Differential kinematics at singular configurations

- Singularities can be also useful though! When?
- Resisting external forces with minimal load in the joints.

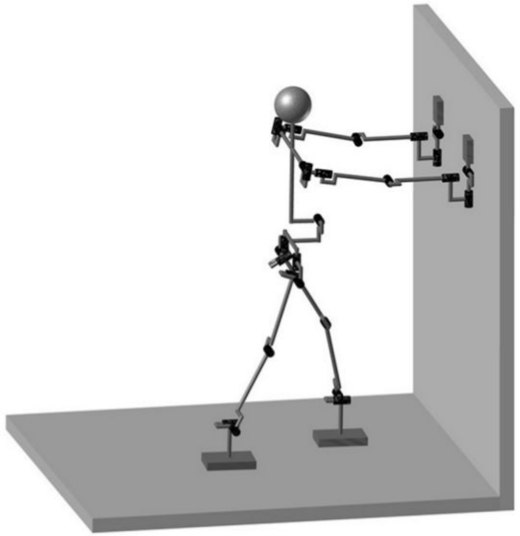

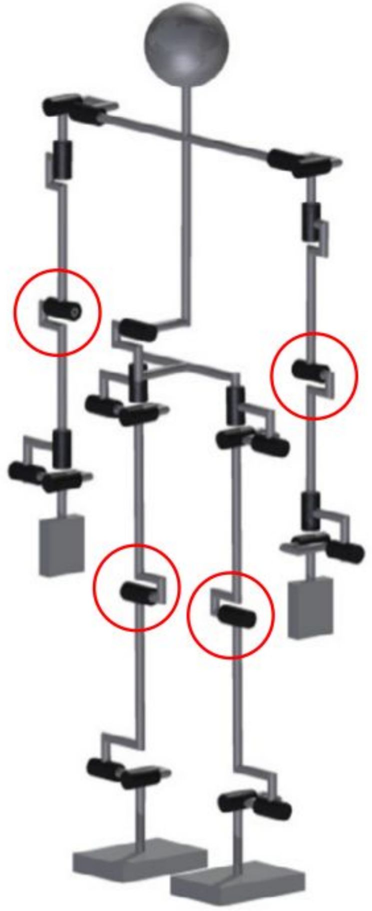

Section 2.5 in Nenchev, D. N., Konno, A., & Tsujita, T. (2018). Humanoid robots: Modeling and control. Butterworth-Heinemann.

Inverse differential kinematic relations

- Given the joint angles and the end-link spatial velocity, find the motion rates in the joints.
- In order to find a solution in a straightforward manner, the following two conditions have to be satisfied:
  a. the Jacobian matrix at branch configuration θ should be of full rank;
  b. the number of joints of the branch should be equal to the DoF of the end link.
- These conditions imply that the inverse of the Jacobian matrix exists.
- When the conditions are satisfied, solving $\mathcal{V}_n = \boldsymbol{J}(\boldsymbol{\theta})\dot{\boldsymbol{\theta}}$ the joint rates yields the following solution to the inverse kinematics problem:

$$\dot{\boldsymbol{\theta}} = \boldsymbol{J}(\boldsymbol{\theta})^{-1}\mathcal{V}$$

- A branch configuration yielding a full-rank Jacobian is called a *nonsingular configuration*.
- A branch with a number of joints that conforms to the second condition is called a kinematically nonredundant branch.

Using J⁻¹ for Cartesian control

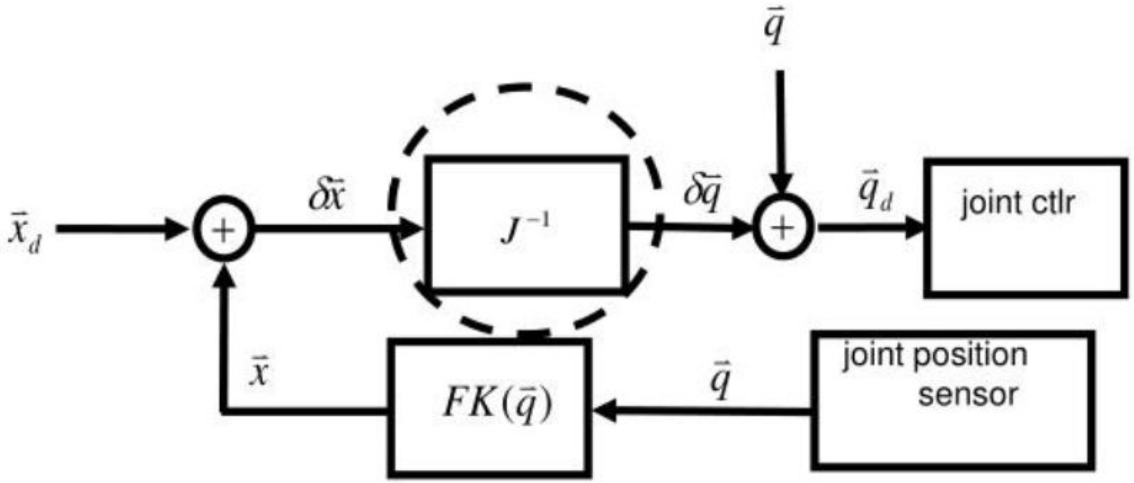

$$\begin{bmatrix}\dot{q}_1\\ \dot{q}_2\end{bmatrix} = J^{-1}\begin{bmatrix}\dot{x}\\ \dot{y}\end{bmatrix}$$

Underactuation, full actuation, and over-actuation

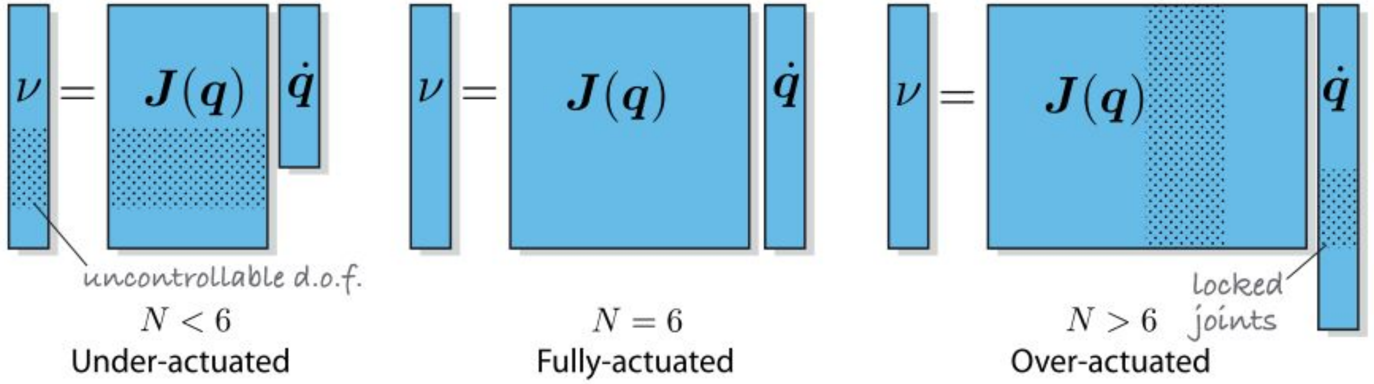

Fig. 8.6 in Corke, P. I. (2013). Robotics, vision and control: fundamental algorithms in MATLAB Berlin: Springer.

$$\dot{\boldsymbol{\theta}} = \boldsymbol{J}(\boldsymbol{\theta})^{-1}\mathcal{V}$$

What if **J(q)** is not square (and full rank) hence the inverse does not exist?

Underactuation

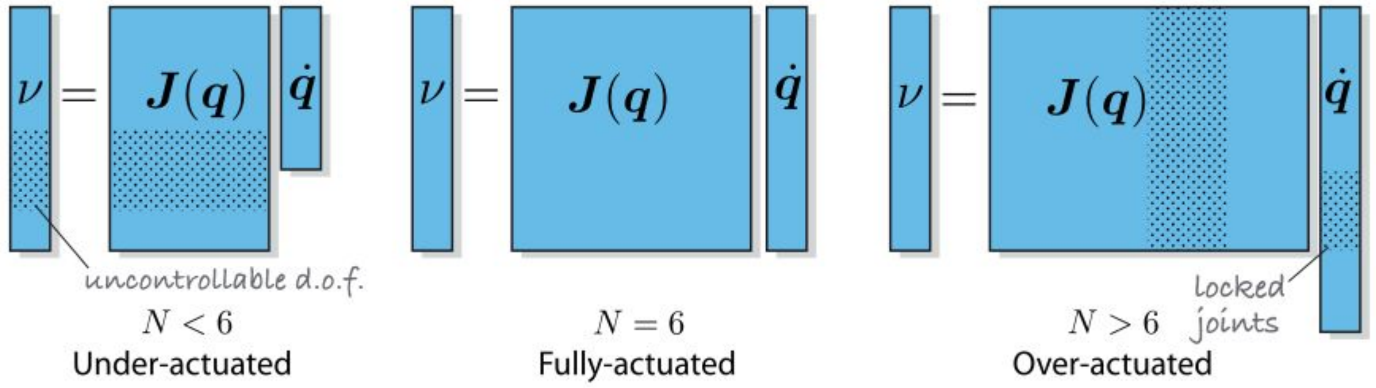

Fig. 8.6 in Corke, P. I. (2013). Robotics, vision and control: fundamental algorithms in MATLAB Berlin: Springer.

n=5, m = 6 (x,y,z, ϕ, θ, ψ)

$$\dot{\theta} = J(\theta)^{-1}\mathcal{V}$$

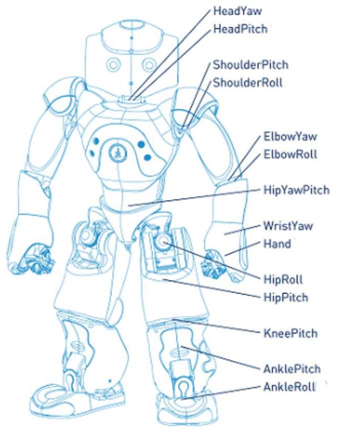

- What if **J(q)** is not square (and full rank) hence the inverse does not exist?
- Underactuated case:
  - Cannot be solved (unless we are lucky) because the system of equations is overdetermined.
  - “Quick hack”: The system can be squared up by deleting some rows of v and J – accepting that some Cartesian degrees of freedom are not controllable given the low number of joints.

Overactuation

Fig. 8.6 in Corke, P. I. (2013). Robotics, vision and control: fundamental algorithms in MATLAB Berlin: Springer.

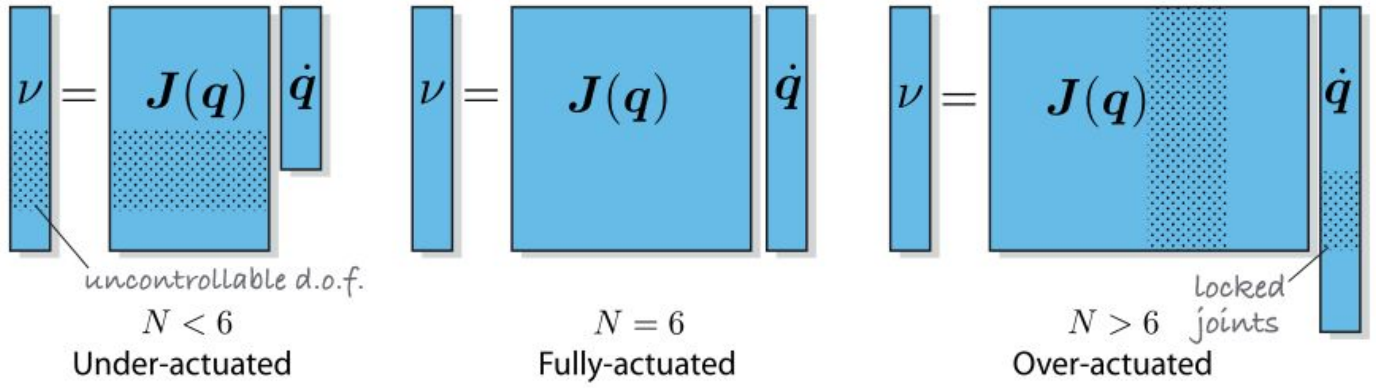

n=7 (or 10), m = 6 (x,y,z, ϕ, θ, ψ)

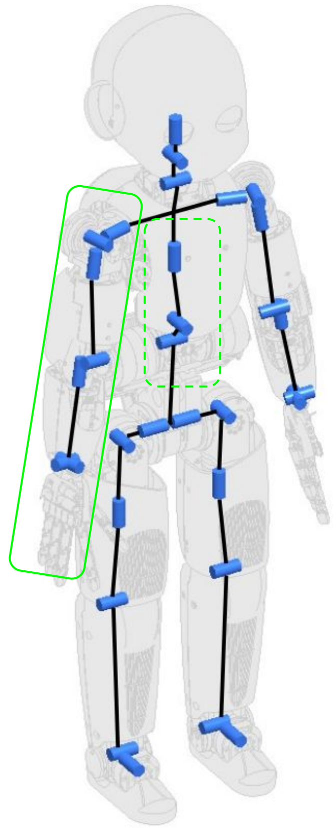

$$\dot{\theta} = J(\theta)^{-1}\mathcal{V}$$

- What if **J(q)** is not square (and full rank) hence the inverse does not exist?
- Overractuated case:
  - The system of equations is underdetermined. Multiple solutions exist and we can find a least squares solution (later).
  - “Quick hack”: Alternatively we can square up the Jacobian to make it invertible by deleting some columns – effectively locking the corresponding axes.
  - What do we do with these extra axes?

Self-motion

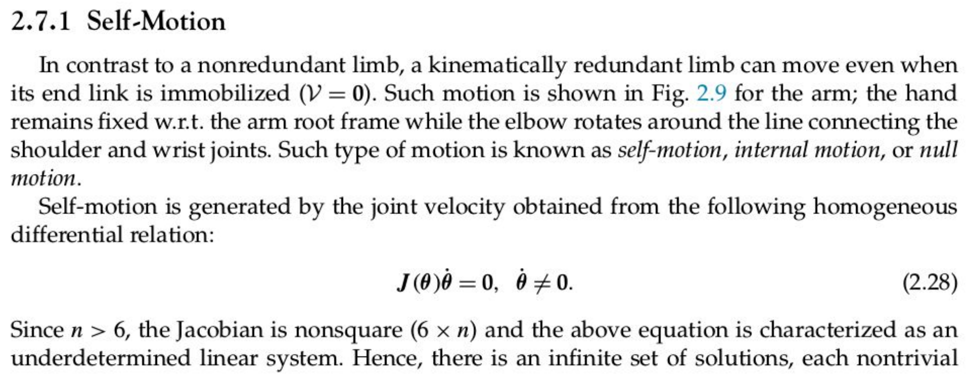

2.7.1 Self-Motion

In contrast to a nonredundant limb, a kinematically redundant limb can move even when its end link is immobilized ($\mathcal{V} = \mathbf{0}$). Such motion is shown in Fig. 2.9 for the arm; the hand remains fixed w.r.t. the arm root frame while the elbow rotates around the line connecting the shoulder and wrist joints. Such type of motion is known as *self-motion*, *internal motion*, or *null motion*.

Self-motion is generated by the joint velocity obtained from the following homogeneous differential relation:

$$\boldsymbol{J}(\boldsymbol{\theta})\dot{\boldsymbol{\theta}} = \mathbf{0}, \quad \dot{\boldsymbol{\theta}} \neq \mathbf{0}. \tag{2.28}$$

Since $n > 6$, the Jacobian is nonsquare ($6 \times n$) and the above equation is characterized as an underdetermined linear system. Hence, there is an infinite set of solutions, each nontrivial

Usage:

- Avoid singularities
- Avoid joint limits
- Avoid obstacles
- Minimize torques
- ...

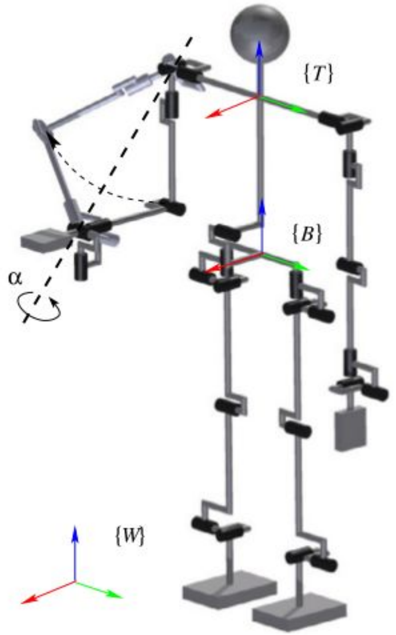

FIGURE 2.9 The self-motion of the arm is shown as a rotation of the arm plane, determined by the upper/lower arm links, around the line connecting the shoulder and wrist joints. The rotation angle α can be associated with parameter b_v in (2.35).

Inverse differential kinematic relations - challenges

- Whenever any of the above two conditions cannot be met, the inverse problem needs to be handled with care.
- Special branch configurations where the Jacobian loses rank. Such configurations are called *singular*.
    - The branch can attain a singular configuration irrespective of the number of its joints.
- Further on, when the branch comprises more joints than the DoF of its end link ($n > 6$), then $\mathcal{V}_n = \boldsymbol{J}(\boldsymbol{\theta})\dot{\boldsymbol{\theta}}$ is underdetermined. This implies the existence of an infinite set of inverse kinematics solutions for the joint rates. In this case, the branch is referred to as a *kinematically redundant branch*.

Generalized inverse

- We are looking for a matrix **J#** such that: $\dot{\theta} = J^{\#}\nu$
- Two cases:
  - Underactuated manipulator (~ overdetermined system of equations): Find $\dot{\theta}$ such that $J\dot{\theta} - \nu$ is minimized.
  - Redundant manipulator (~ underdetermined system of equations): Find $\dot{\theta}$ solving $\nu = J\dot{\theta}$ optimizing some additional property.

Using differential kinematics for IK

- They are numerical, iterative methods.
    - Jacobian transpose
    - Jacobian pseudoinverse
    - Damped least squares

More details in

- Buss, S. R. (2004). Introduction to inverse kinematics with Jacobian transpose, pseudoinverse and damped least squares methods. IEEE Journal of Robotics and Automation, 17(1-19), 16.
- 2.7.2 - 2.7.5 in Nenchev et al. (2018)
- Jacobian transpose - duality of kinematics and statics - 8.4 in Corke, P. I. (2013). Robotics, vision and control: fundamental algorithms in MATLAB Berlin: Springer.
- https://github.com/vvv-school/vvv18/blob/master/material/kinematics/kinematics.pdf
- Howie Choset: https://www.slideserve.com/antonia/inverting-the-jacobian-and-manipulability

Jacobian transpose

We aim to minimize the Cartesian error: $g = \frac{1}{2}\|\mathbf{e}\|^2 = \frac{1}{2}\|\mathbf{x}_d - \mathbf{f}(\mathbf{q})\|^2$

Compute the gradient: $\nabla_{\mathbf{q}} g = \frac{1}{2}\nabla_{\mathbf{q}}\left\langle(\mathbf{x}_d - \mathbf{f}),(\mathbf{x}_d - \mathbf{f})\right\rangle = \frac{1}{2}\cdot\left(-2\left\langle\nabla_{\mathbf{q}}\mathbf{f},(\mathbf{x}_d - \mathbf{f})\right\rangle\right) =$

$$= -\left\langle\mathbf{J},(\mathbf{x}_d - \mathbf{f})\right\rangle = -\mathbf{J}^T(\mathbf{x}_d - \mathbf{f}) = -\mathbf{J}^T\mathbf{e}$$

Gradient descent method for system of nonlinear equations: $\dot{\mathbf{q}} = \mathbf{K}\cdot\left(-\nabla_{\mathbf{q}} g\right) = \mathbf{J}^T\mathbf{K}\mathbf{e}$

we only employ *direct kinematics functions*!

Jacobian transpose from statics

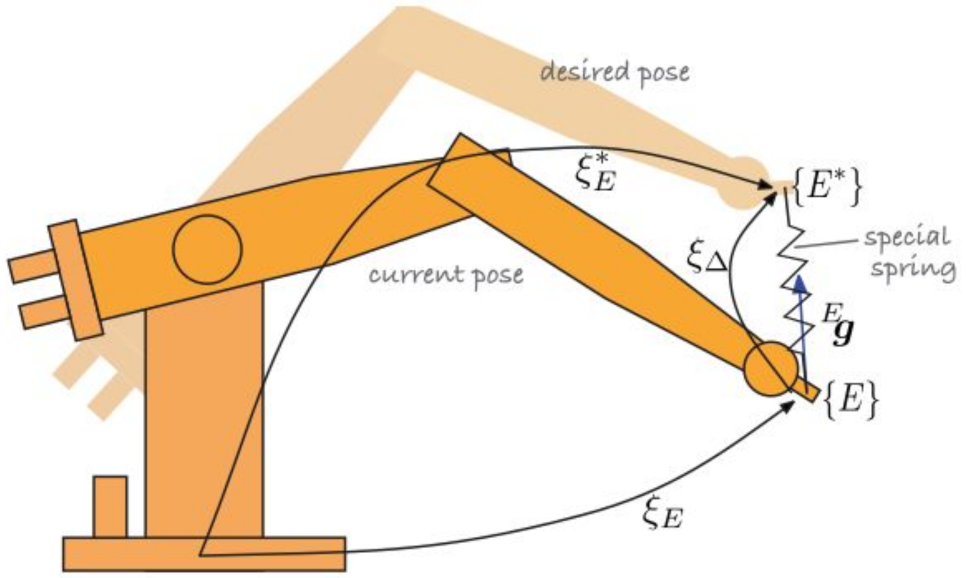

Fig. 8.7.
Schematic of the numerical inverse kinematic approach, showing the current ξ_E and the desired ξ_E^* manipulator pose

8.4 in Corke, P. I. (2013). Robotics, vision and control: fundamental algorithms in MATLAB Berlin: Springer.

Jacobian pseudoinverse

redundant chain $n > m$

Reformulate the problem as a *linear constrained optimization*

$$\dot{\mathbf{q}}^* = \arg\min_{\dot{\mathbf{q}}} \left(\frac{1}{2} \dot{\mathbf{q}}^T \mathbf{W} \dot{\mathbf{q}} \right)$$

$$\text{s.t.} \quad \dot{\mathbf{x}} = \mathbf{J}\dot{\mathbf{q}}$$

Recruit Lagrangian multipliers:

$$\dot{\mathbf{q}}^* = \arg\min_{\dot{\mathbf{q}},\lambda} \left(\frac{1}{2} \dot{\mathbf{q}}^T \mathbf{W} \dot{\mathbf{q}} + \lambda^T \left(\dot{\mathbf{x}} - \mathbf{J}\dot{\mathbf{q}} \right) \right)$$

$$\dot{\mathbf{q}}^* = \mathbf{W}^{-1}\mathbf{J}^T \left(\mathbf{J}\mathbf{W}^{-1}\mathbf{J}^T \right)^{-1} \dot{\mathbf{x}}$$

$$\begin{cases} \mathbf{W} = \mathbf{I}_n \\ \mathbf{J}^\dagger = \mathbf{J}^T \left(\mathbf{J}\mathbf{J}^T \right)^{-1} \quad \Rightarrow \quad \dot{\mathbf{q}} = \mathbf{J}^\dagger \dot{\mathbf{x}} \\ \mathbf{J}\mathbf{J}^\dagger = \mathbf{I}_n \end{cases}$$

https://github.com/vvv-school/vvv18/blob/master/material/kinematics/kinematics.pdf, courtesy Ugo Pattacini

Psuedoinverse definition: (underconstrained)

Given a desired twist, $\dot{x}_d$, find a vector of joint velocities, $\dot{q}$, that satisfies $\dot{x}_d = J\dot{q}$ while minimizing $f(\dot{q}) = \dot{q}^T \dot{q}$

Minimize joint velocities

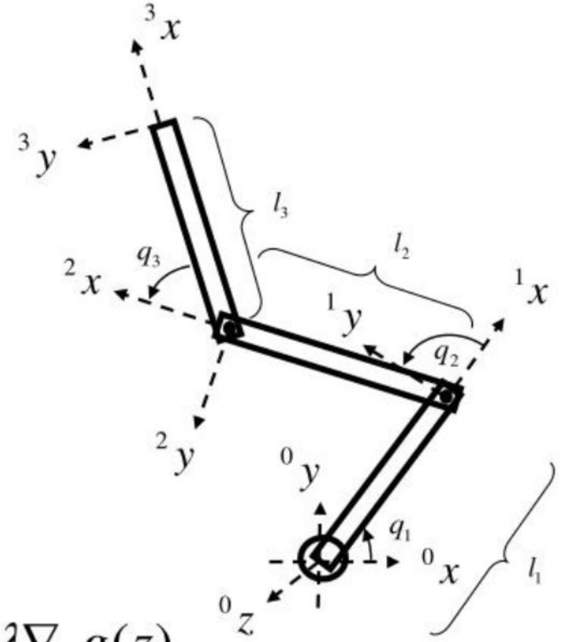

Minimize $f(z)$ subject to $g(z) = 0$:

Use **lagrange multiplier method**: $\nabla_z f(z) = \lambda \nabla_z g(z)$

This condition must be met when $f(z)$ is at a minimum subject to $g(z) = 0$

$$\nabla_z f(z) = \lambda \nabla_z g(z)$$

$$f(\dot{q}) = \tfrac{1}{2}\dot{q}^T \dot{q} \longleftarrow \text{Minimize}$$

$$g(\dot{q}) = J\dot{q} - \dot{x} = 0 \longleftarrow \text{Subject to}$$

$$\nabla_{\dot{q}} f(\dot{q}) = \dot{q}^T$$

$$\nabla_{\dot{q}} g(\dot{q}) = J$$

$$\dot{q}^T = \lambda^T J$$

$$\dot{q} = J^T \lambda$$

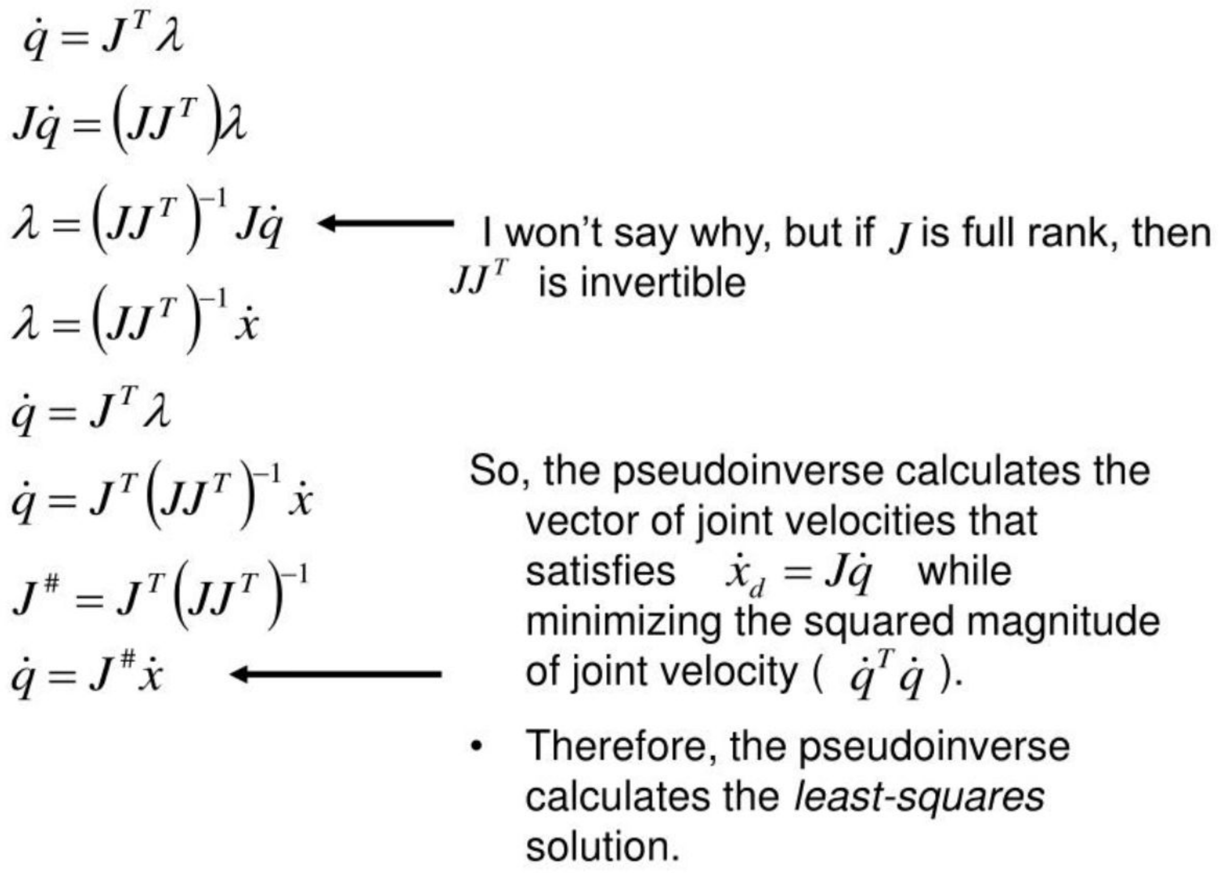

$$\dot{q} = J^T \lambda$$

$$J\dot{q} = \left(JJ^T\right)\lambda$$

$$\lambda = \left(JJ^T\right)^{-1} J\dot{q} \longleftarrow$$

I won't say why, but if J is full rank, then JJ^T is invertible

$$\lambda = \left(JJ^T\right)^{-1} \dot{x}$$

$$\dot{q} = J^T \lambda$$

$$\dot{q} = J^T\left(JJ^T\right)^{-1} \dot{x}$$

$$J^{\#} = J^T\left(JJ^T\right)^{-1}$$

$$\dot{q} = J^{\#}\dot{x} \longleftarrow$$

So, the pseudoinverse calculates the vector of joint velocities that satisfies $\dot{x}_d = J\dot{q}$ while minimizing the squared magnitude of joint velocity ($\dot{q}^T \dot{q}$).

- Therefore, the pseudoinverse calculates the *least-squares* solution.

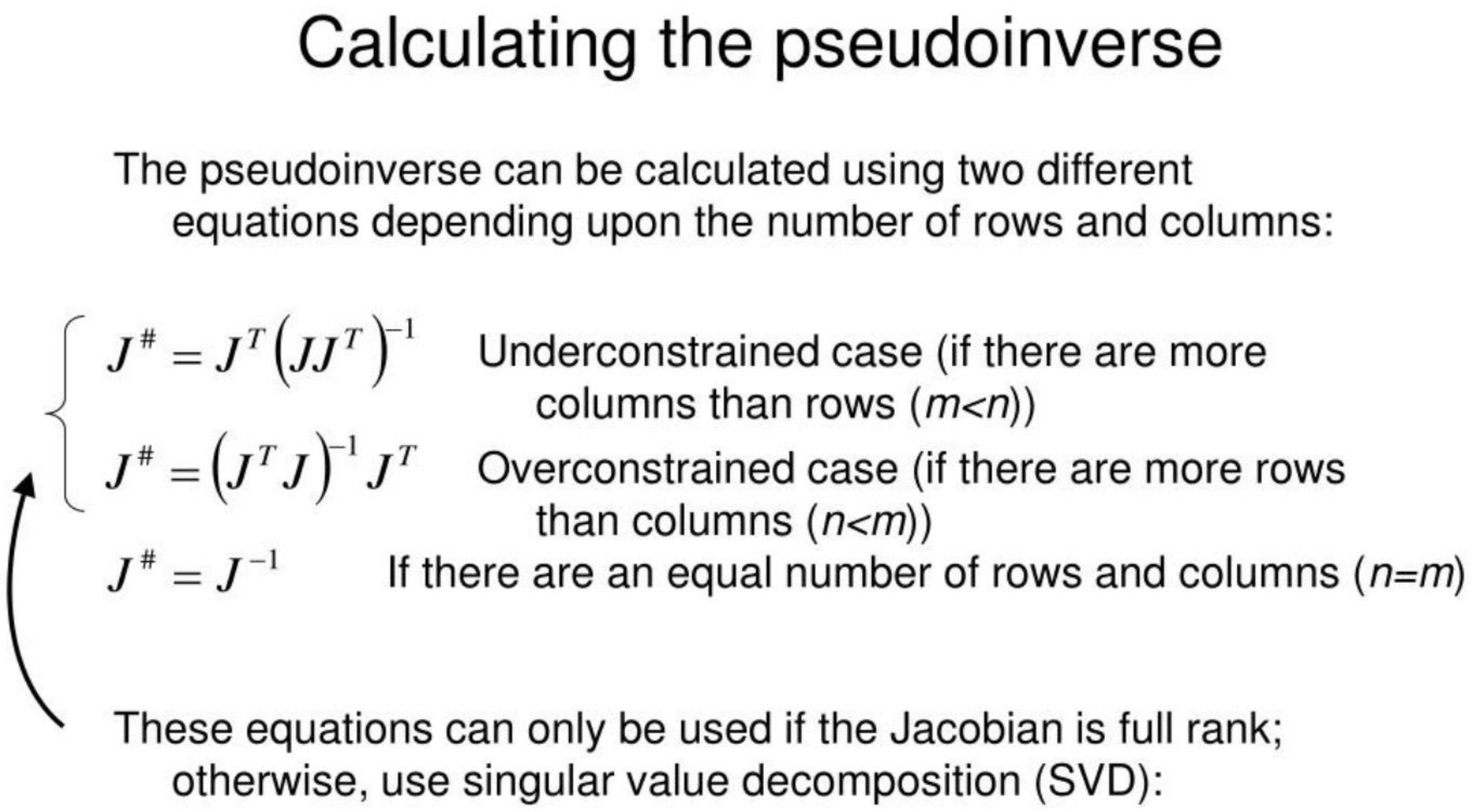

Calculating the pseudoinverse

The pseudoinverse can be calculated using two different equations depending upon the number of rows and columns:

$$J^{\#} = J^{T}\left(JJ^{T}\right)^{-1}$$

Underconstrained case (if there are more columns than rows ($m<n$))

$$J^{\#} = \left(J^{T}J\right)^{-1}J^{T}$$

Overconstrained case (if there are more rows than columns ($n<m$))

$$J^{\#} = J^{-1}$$

If there are an equal number of rows and columns ($n=m$)

These equations can only be used if the Jacobian is full rank; otherwise, use singular value decomposition (SVD):

Howie Choset: https://www.slideserve.com/antonia/inverting-the-jacobian-and-manipulability

Calculating the pseudoinverse using SVD

Singular value decomposition decomposes a matrix as follows:

$$J = \underbrace{U}_{m\times m}\underbrace{\Sigma}_{m\times n}\underbrace{V^T}_{n\times n}$$

Σ is a diagonal matrix of singular values:

$$J = U\begin{bmatrix} \sigma_1 & 0 & 0 & 0 & 0 & 0 & 0 \\ 0 & \sigma_2 & 0 & 0 & 0 & 0 & 0 \\ 0 & 0 & \sigma_3 & 0 & 0 & 0 & 0 \\ 0 & 0 & 0 & \ddots & 0 & 0 & 0 \\ 0 & 0 & 0 & 0 & \sigma_n & 0 & 0 \end{bmatrix}V^T$$

~ manipulability (velocity) ellipsoid

$$J^{\#} = V\Sigma^{-1}U^T$$

$$J^{\#} = V\begin{bmatrix} \frac{1}{\sigma_1} & 0 & 0 & 0 & 0 \\ 0 & \frac{1}{\sigma_2} & 0 & 0 & 0 \\ 0 & 0 & \frac{1}{\sigma_3} & 0 & 0 \\ 0 & 0 & 0 & \ddots & 0 \\ 0 & 0 & 0 & 0 & \frac{1}{\sigma_n} \\ 0 & 0 & 0 & 0 & 0 \\ 0 & 0 & 0 & 0 & 0 \end{bmatrix}U^T$$

~ force ellipsoid

Velocity and force manipulability are orthogonal!

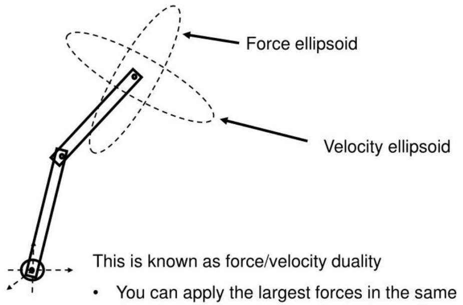

This is known as force/velocity duality

- You can apply the largest forces in the same directions that your max velocity is smallest
- Your max velocity is greatest in the directions where you can only apply the smallest forces

Howie Choset: https://www.slideserve.com/antonia/inverting-the-jacobian-and-manipulability

Properties of the pseudoinverse

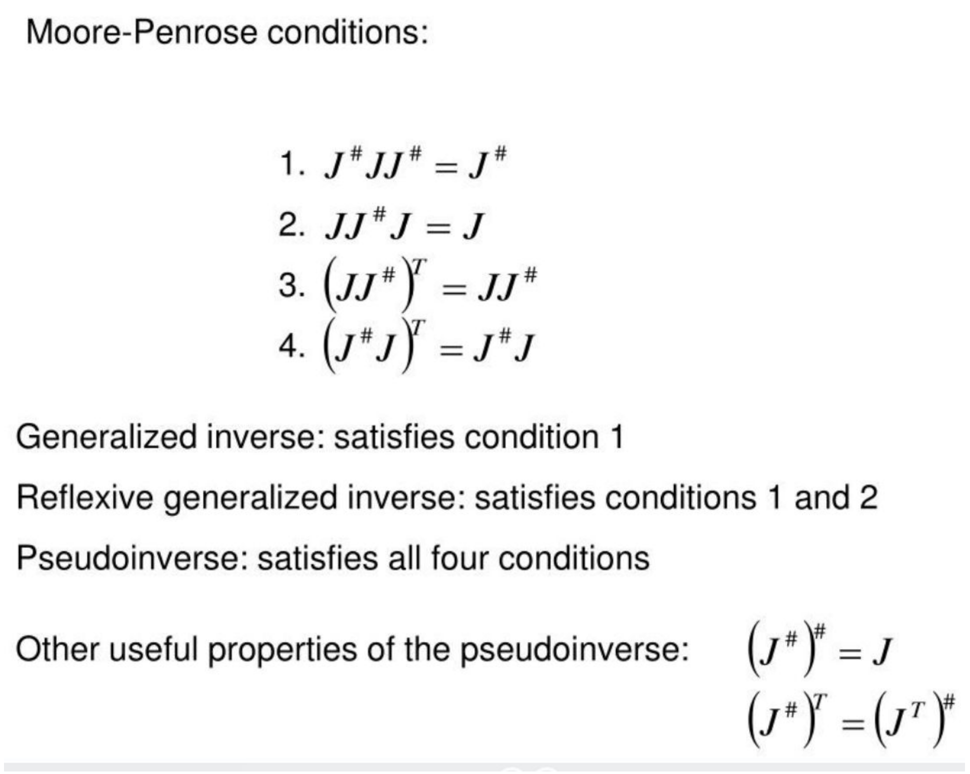

Moore-Penrose conditions:

1. $J^{\#}JJ^{\#} = J^{\#}$
2. $JJ^{\#}J = J$
3. $\left(JJ^{\#}\right)^T = JJ^{\#}$
4. $\left(J^{\#}J\right)^T = J^{\#}J$

Generalized inverse: satisfies condition 1

Reflexive generalized inverse: satisfies conditions 1 and 2

Pseudoinverse: satisfies all four conditions

Other useful properties of the pseudoinverse:

$$\left(J^{\#}\right)^{\#} = J$$

$$\left(J^{\#}\right)^T = \left(J^T\right)^{\#}$$

Secondary task

redundant chain $n > m$

Reformulate the problem as a *linear constrained optimization*

$$\dot{\mathbf{q}}^* = \arg\min_{\dot{\mathbf{q}}} \left(\frac{1}{2} (\dot{\mathbf{q}} - \dot{\mathbf{q}}_0)^T (\dot{\mathbf{q}} - \dot{\mathbf{q}}_0) \right)$$

$$\text{s.t.} \quad \dot{\mathbf{x}} = \mathbf{J}\dot{\mathbf{q}}$$

$$\Downarrow$$

$$\dot{\mathbf{q}} = \mathbf{J}^\dagger \dot{\mathbf{x}} + \left(\mathbf{I}_n - \mathbf{J}^\dagger \mathbf{J} \right) \dot{\mathbf{q}}_0$$

$$\dot{\mathbf{q}} = \dot{\mathbf{q}}_0 + \mathbf{J}^\dagger \left(\dot{\mathbf{x}} - \mathbf{J}\dot{\mathbf{q}}_0 \right)$$

$\left(\mathbf{I}_n - \mathbf{J}^\dagger \mathbf{J} \right)$ Null-space projection operator allows for *internal motions*

How to pick up $\dot{q}_0$:
$$\dot{\mathbf{q}}_0 = k_0 \left(\frac{\partial w(\mathbf{q})}{\partial \mathbf{q}} \right)^T$$

Improve manipulability
$$w(\mathbf{q}) = \sqrt{\det\left(\mathbf{J}(\mathbf{q}) \mathbf{J}^T(\mathbf{q}) \right)}$$

Joint limits avoidance
$$w(\mathbf{q}) = -\frac{1}{2n} \sum_{i=1}^{n} \left(\frac{q_i - \bar{q}_i}{q_{iM} - q_{im}} \right)^2$$

Using J$^{\#}$ for Cartesian control

Position

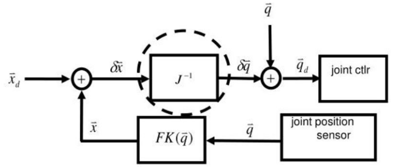

$$\begin{bmatrix} \dot{q}_1 \\ \dot{q}_2 \end{bmatrix} = J^{-1} \begin{bmatrix} \dot{x} \\ \dot{y} \end{bmatrix}$$

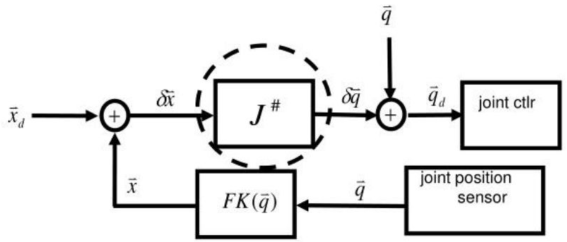

Procedure for controlling position:

1. Calculate position error: x_{err}
2. Multiply by a scaling factor: $\delta x_{err} = \alpha x_{err}$
3. Multiply by the velocity Jacobian pseudoinverse: $\dot{q} = J_v^{\#} \alpha x_{err}$

Orientation

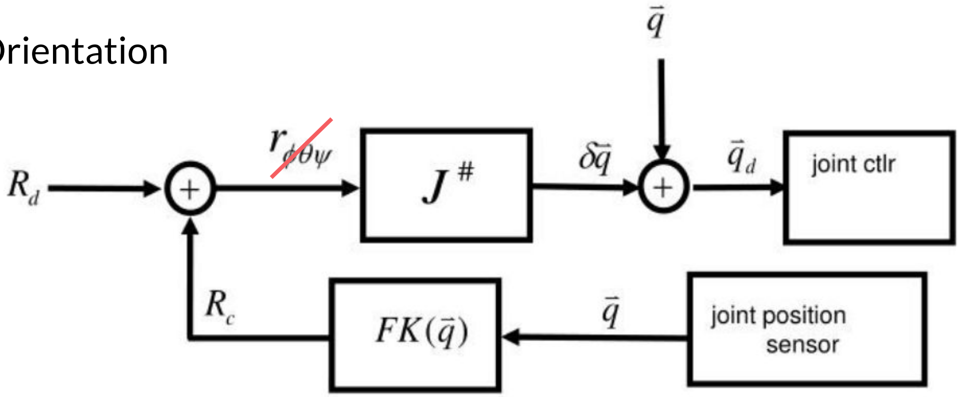

Remember that in general: $J_\omega \neq \dfrac{\partial r_{\phi\theta\psi}}{\partial q}$

Use analytical Jacobian or axis-angle representation and Rodrigues formula. (mechanical vs. representational singularities…)

See slides 16-20 in
https://www.slideserve.com/antonia/inverting-the-jacobian-and-manipulability

Jacobian transpose vs. pseudoinverse

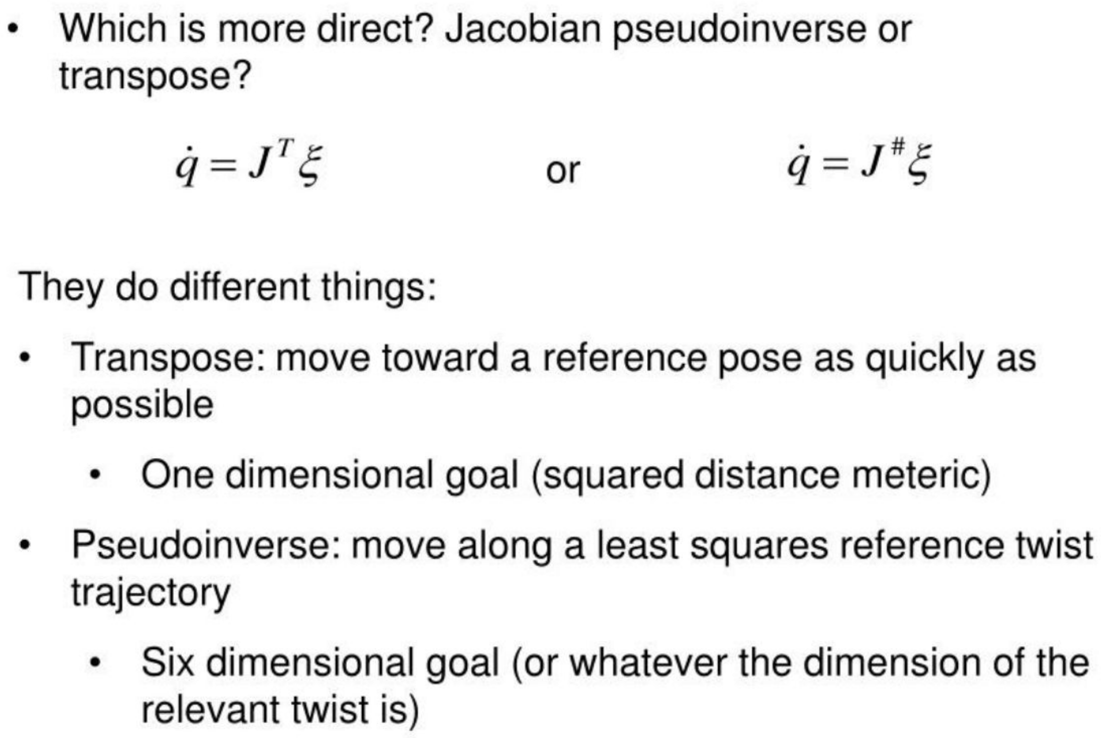

- Which is more direct? Jacobian pseudoinverse or transpose?

$$\dot{q} = J^T \xi \qquad \text{or} \qquad \dot{q} = J^{\#} \xi$$

They do different things:

- Transpose: move toward a reference pose as quickly as possible
  - One dimensional goal (squared distance meteric)
- Pseudoinverse: move along a least squares reference twist trajectory
  - Six dimensional goal (or whatever the dimension of the relevant twist is)

Howie Choset: https://www.slideserve.com/antonia/inverting-the-jacobian-and-manipulability

Jacobian transpose vs. pseudoinverse

The pseudoinverse moves the end effector in a straight line path toward the goal pose using the least squared joint velocities.

- The goal is specified in terms of the reference twist
- Manipulator follows a straight line path in Cartesian space

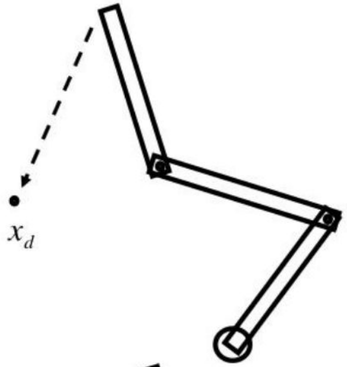

The transpose moves the end effector toward the goal position

- In general, not a straight line path *in Cartesian space*
- Instead, the transpose follows the gradient in *joint space*

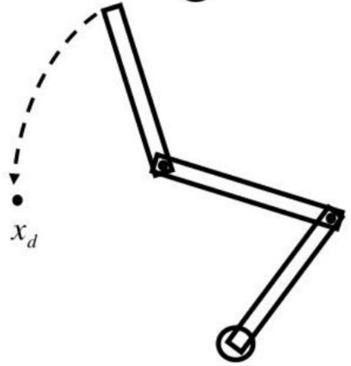

Damped Least Squares

To deal with kinematic singularities

$$\dot{\mathbf{q}}^* = \arg\min_{\dot{\mathbf{q}}} \left(\frac{1}{2} (\dot{\mathbf{x}} - \mathbf{J}\dot{\mathbf{q}})^T (\dot{\mathbf{x}} - \mathbf{J}\dot{\mathbf{q}}) + \frac{1}{2} k^2 \dot{\mathbf{q}}^T \dot{\mathbf{q}} \right)$$

$$\Downarrow$$

Levenberg-Marquardt method
for system of nonlinear equations

$$\mathbf{J}^* = \mathbf{J}^T \left(\mathbf{J}\mathbf{J}^T + k^2 \mathbf{I}_n \right)^{-1}$$

$$\dot{\mathbf{q}} = \mathbf{J}^* \dot{\mathbf{x}}$$

k establishes a synergy between:

- Jacobian (Pseudo-)inverse: $k = 0$
- Jacobian Transpose: $k \gg \max\{|\sigma_i|\}$

https://github.com/vvv-school/vvv18/blob/master/material/kinematics/kinematics.pdf, courtesy Ugo Pattacini

Using differential kinematics for IK

Iterative Methods

https://github.com/vvv-school/vvv18/blob/master/material/kinematics/kinematics.pdf, courtesy Ugo Pattacini

Jacobian Transpose $\dot{\mathbf{q}} = \mathbf{J}^T\mathbf{K}\mathbf{e}, \quad \mathbf{e} = \mathbf{x}_d - \mathbf{x}_e$

Jacobian Pseudoinverse $\dot{\mathbf{q}} = \mathbf{J}^\dagger\mathbf{K}\mathbf{e} + \left(\mathbf{I} - \mathbf{J}^\dagger\mathbf{J}\right)\dot{\mathbf{q}}_0, \quad \mathbf{J}^\dagger = \mathbf{J}^T\left(\mathbf{J}\mathbf{J}^T\right)^{-1}$

Damped Least Squares $\dot{\mathbf{q}} = \mathbf{J}^*\mathbf{K}\mathbf{e}, \quad \mathbf{J}^* = \mathbf{J}^T\left(\mathbf{J}\mathbf{J}^T + k^2\mathbf{I}\right)^{-1}$

- More details in
  - Buss, S. R. (2004). Introduction to inverse kinematics with Jacobian transpose, pseudoinverse and damped least squares methods. IEEE Journal of Robotics and Automation, 17(1-19), 16.
  - 2.7.2 - 2.7.5 in Nenchev et al. (2018); Redundancy resolution 2.7.4-2.7.5
  - Jacobian transpose - duality of kinematics and statics - 8.4 in Corke, P. I. (2013). Robotics, vision and control: fundamental algorithms in MATLAB Berlin: Springer.
  - https://github.com/vvv-school/vvv18/blob/master/material/kinematics/kinematics.pdf
  - Howie Choset: https://www.slideserve.com/antonia/inverting-the-jacobian-and-manipulability

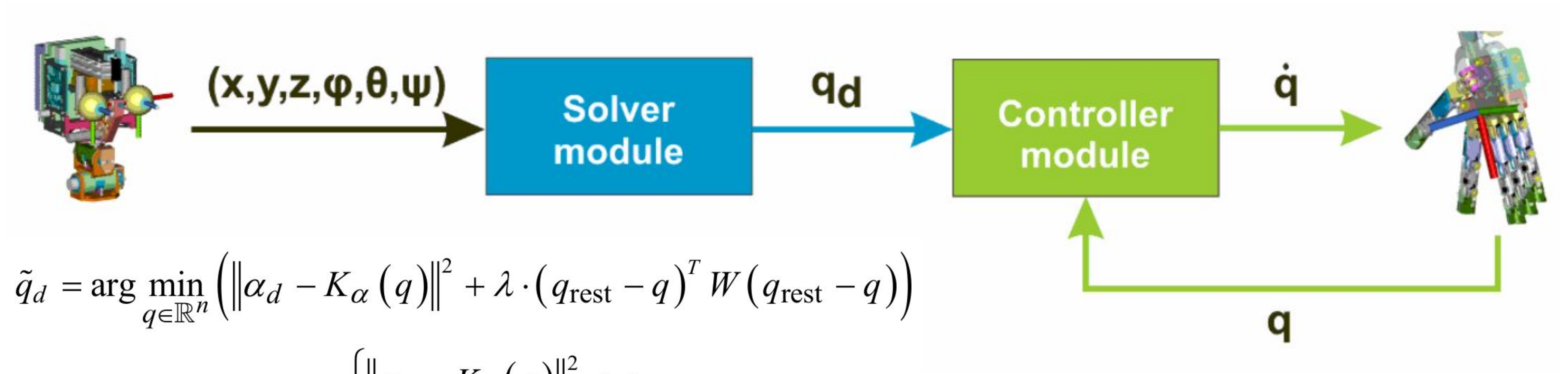

$$\tilde{q}_d = \arg\min_{q\in\mathbb{R}^n}\left(\left\|\alpha_d - K_\alpha(q)\right\|^2 + \lambda\cdot\left(q_{\text{rest}} - q\right)^T W\left(q_{\text{rest}} - q\right)\right)$$

$$\text{s.t.}\begin{cases}\left\|x_d - K_x(q)\right\|^2 < \varepsilon \\ q_L < q < q_U \\ \text{other obstacles ...}\end{cases}$$

- **Quick convergence**: real-time compliant, < **20 ms**
- **Scalability**: *n* can be high and set on the fly
- **Singularities handling**: no Jacobian inversion
- **Joints bound handling**: no explicit boundary functions
- **Tasks hierarchy**: no use of null space
- **Complex constraints**: intrinsically nonlinear

https://github.com/vvv-school/vvv18/blob/master/material/kinematics/kinematics.pdf, courtesy Ugo Pattacini

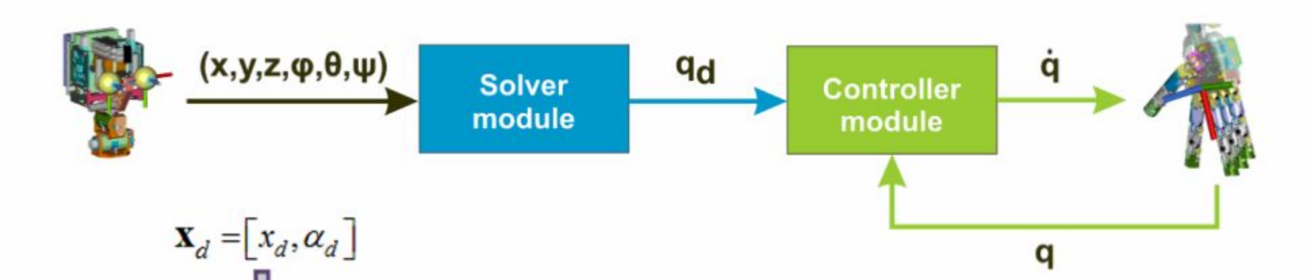

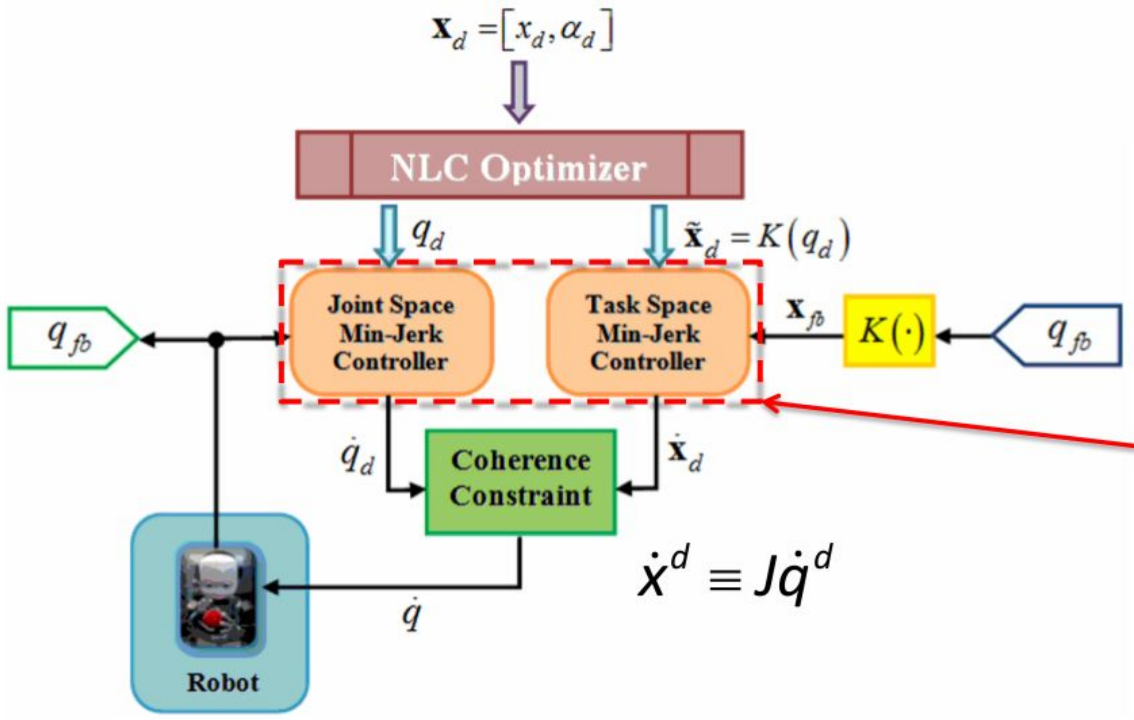

$$\dot{x}^d \equiv J\dot{q}^d$$

Multi Referential Dynamical Systems

M. Hersch, A.G. Billard, "*Reaching with multi-referential dynamical systems*", Springer-Verlag.

Reactive velocity controller with whole-body obstacle avoidance

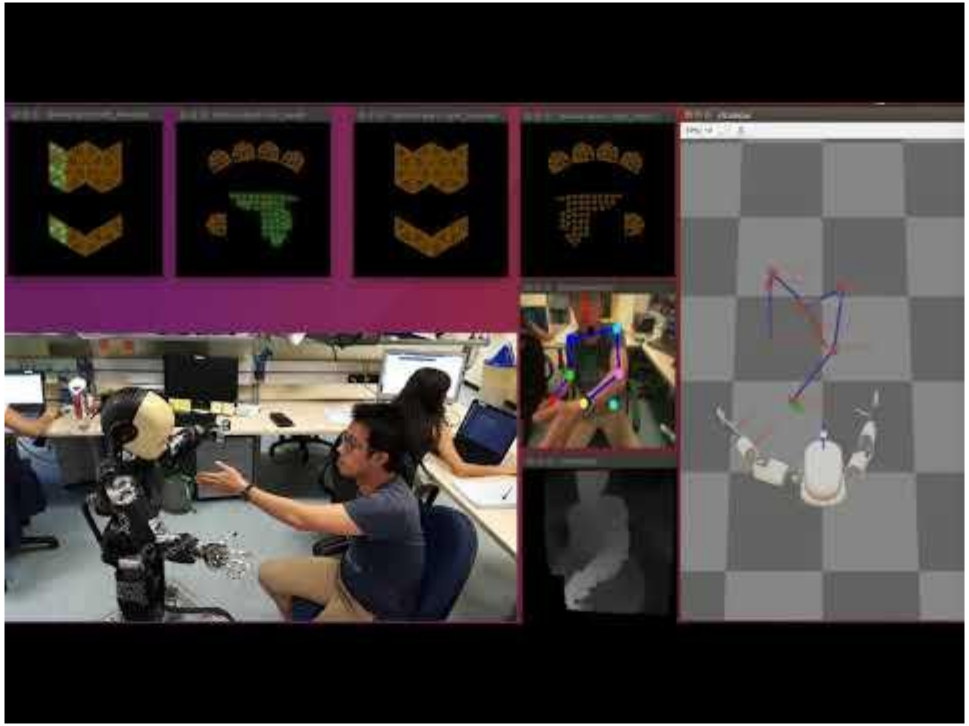

Nguyen, P. D.; Hoffmann, M.; Roncone, A.; Pattacini, U. & Metta, G. (2018), Compact real-time avoidance on a humanoid robot for human-robot interaction, *in* 'HRI '18: 2018 ACM/IEEE International Conference on Human-Robot Interaction', ACM, New York, NY, USA, pp. 416-424.[ACM digital library][arxiv]

New reaching controller

- Previously: iCub inverse kinematics solver and Cartesian controller decoupled (Pattacini et al. 2010)
- Now: single velocity solver + controller

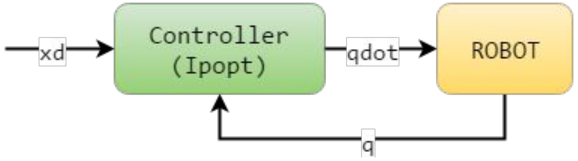

$$\dot{\mathbf{q}}_d = \arg\min_{\dot{\mathbf{q}} \in \mathbb{R}^n} \left(\left\| \overline{\mathbf{x}}_{EEd} - \left(\overline{\mathbf{x}}_{EE} + T_S \mathbf{J}(\overline{\mathbf{q}}) \dot{\mathbf{q}} \right) \right\|^2 \right)$$

$$\text{s.t.} \begin{cases} \mathbf{q}_L < \overline{\mathbf{q}} + T_S \dot{\mathbf{q}} < \mathbf{q}_U \\ \dot{\mathbf{q}}_L < \dot{\mathbf{q}} < \dot{\mathbf{q}}_U \\ \text{other constraints...} \end{cases}$$

$$\xrightarrow{\textit{obstacles}}$$

$$\begin{cases} \mathbf{s} = -\mathbf{J}_C^T \mathbf{n}_C \cdot V_C \cdot a_{PPS} \\ \dot{q}_{L,i} = \max\left\{ V_{L,i}, s_i \right\} \quad s_i > 0 \\ \dot{q}_{U,i} = \min\left\{ V_{U,i}, s_i \right\} \quad s_i < 0 \end{cases}$$

- **Local constrained minimization** @ each instant $\bar{t}$ of Cartesian distances with one-step look-ahead $\bar{t} + T_S$
- Search space: **joint velocities**
- **Fast convergence**, can run @ $T_S \leq 10$ ms
- Use of consolidated optimization library: **Ipopt**

Reaching Controller: Obstacles

- Mapping multiple Cartesian obstacles / repulsive vectors onto joint velocity limits to bring about avoidance

$$\begin{cases} \mathbf{s} = -\mathbf{J}_C^T \mathbf{n}_C \cdot V_C \cdot a_{PPS} \\ \dot{q}_{L,i} = \max\left\{V_{L,i}, s_i\right\} \quad s_i > 0 \\ \dot{q}_{U,i} = \min\left\{V_{U,i}, s_i\right\} \quad s_i < 0 \end{cases}$$

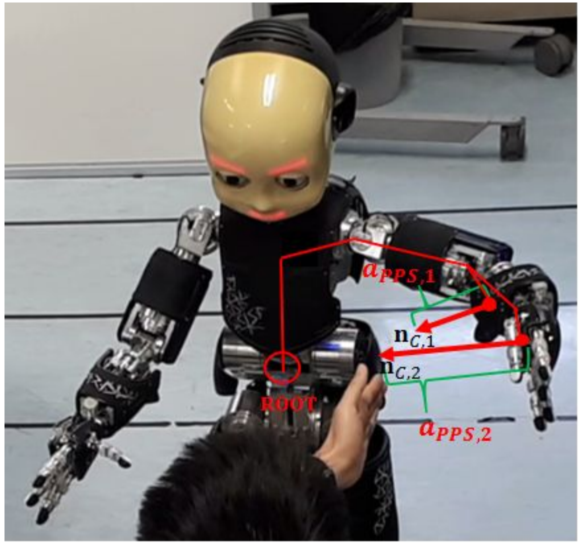

- Control points (C) – loci of PPS activations
- V_C – gain factor for avoidance
- a_{PPS} – PPS activation
- V_L, V_U – bounding values of joint velocity
- s_j - degree of influence of the Cartesian constraint on the *j-th* joint

static target

& simultaneous
obstacle avoidance

moving target

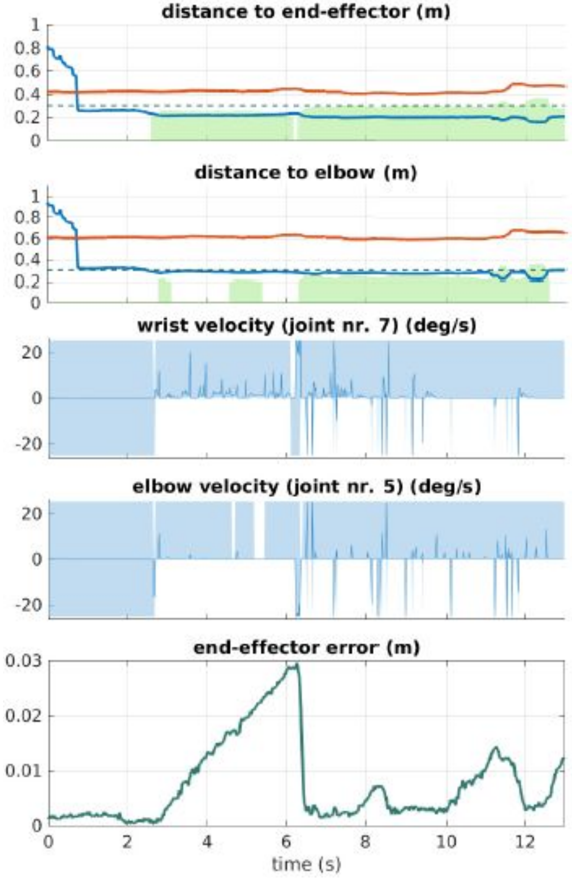

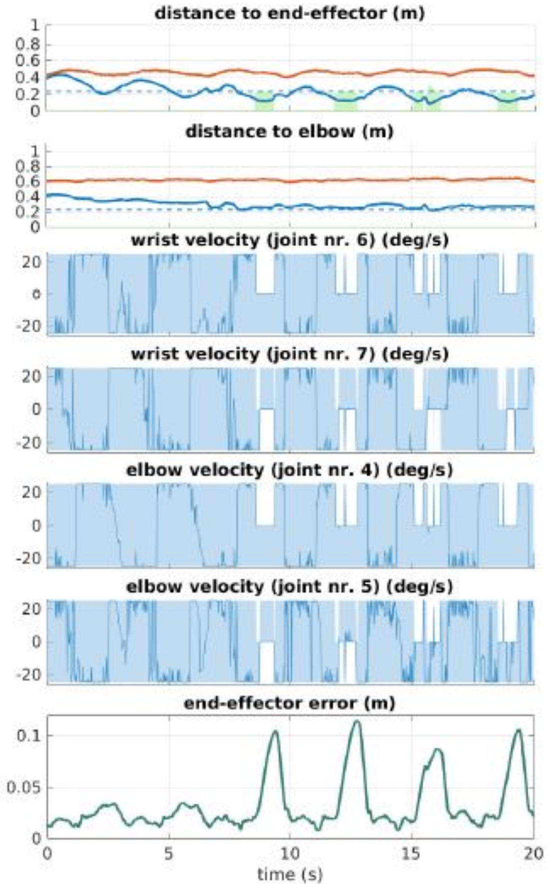

Inverse kinematics for humanoids

(a bit speculative)

There's no free lunch...

Method	General solution (not robot specific)	Possibility of including additional constraints	Problems with singularities	Problems with local minima	Runtime	Examples
Analytical (closed-form)	😞	😑	😑	😌	😄	
Iterative using some form of Jacobian inverse	😌	😞	😞 (not DLS)	😑	😌	KDL / Orocos (ROS)
Optimization using forward kinematics	😌	😑	😌	😑	😌	iCub IK solver, iCub reactive controller

Gaze control

https://youtu.be/I4ZKfAvs1y0

https://youtu.be/_dPlkFPowCc?t=35

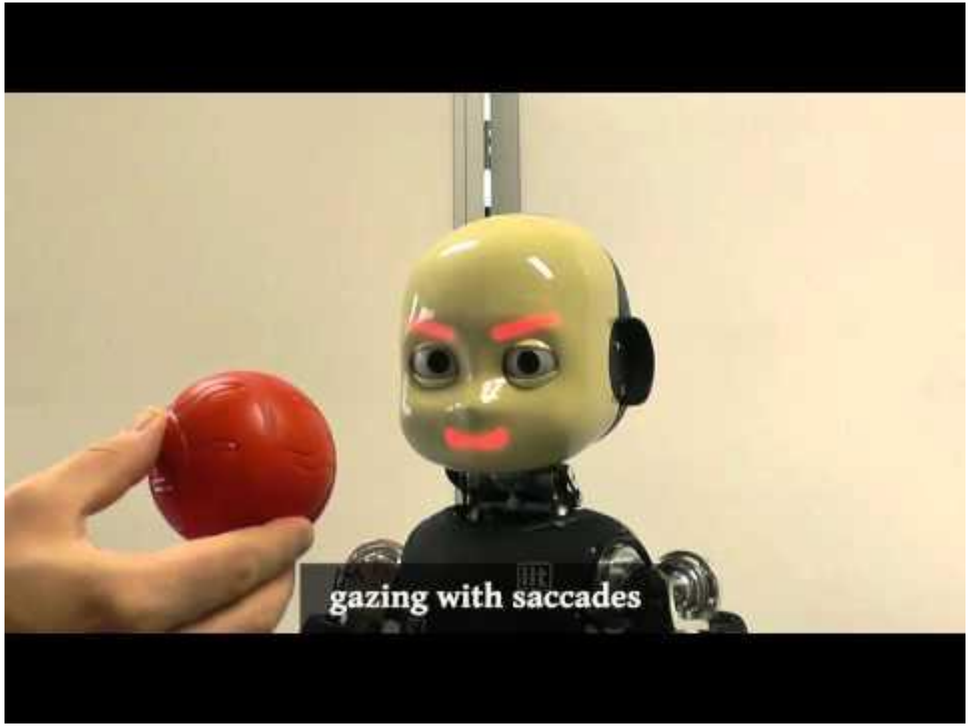

Roncone, A., Pattacini, U., Metta, G., & Natale, L. (2016, June). A Cartesian 6-DoF Gaze Controller for Humanoid Robots. In *Robotics: Science and Systems* (Vol. 2016).

Gaze control

- What kind of inverse kinematics problem is it?
- How many DoF in joint space?
- How many DoF for the task?
- What can the redundancy be used for?

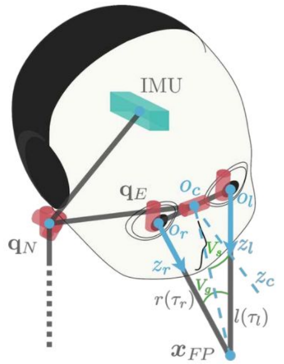

Joint #	Part	Joint Name	Range	Unit
0	Neck	**Pitch**	+/−	[deg]
1	Neck	**Roll**	+/−	[deg]
2	Neck	**Yaw**	+/−	[deg]
3	Eyes	**Tilt**	+/−	[deg]
4	Eyes	**Version**	+/−	[deg]
5	Eyes	**Vergence**	≥ 0	[deg]

iCub gaze controller

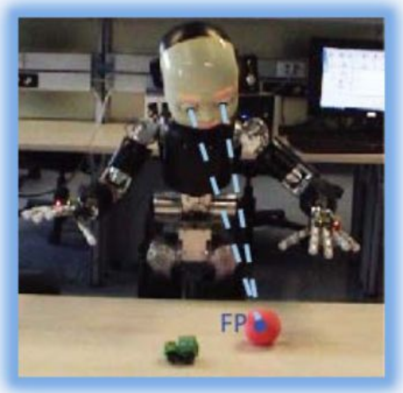

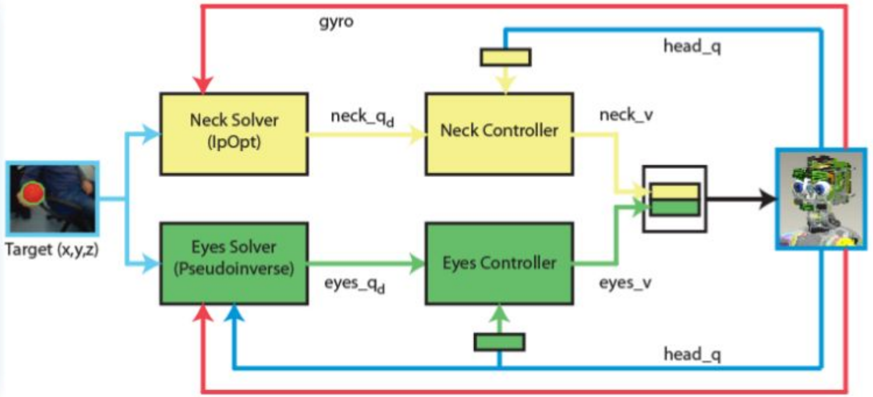

Yet another Cartesian Controller: **reuse ideas** …

Then, apply easy transformations from Cartesian to …

1. Egocentric angular space
2. Image planes (mono and stereo)

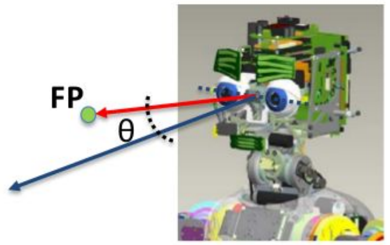

https://github.com/vvv-school/vvv18/blob/master/material/kinematics/kinematics.pdf, courtesy Ugo Pattacini

iCub gaze controller

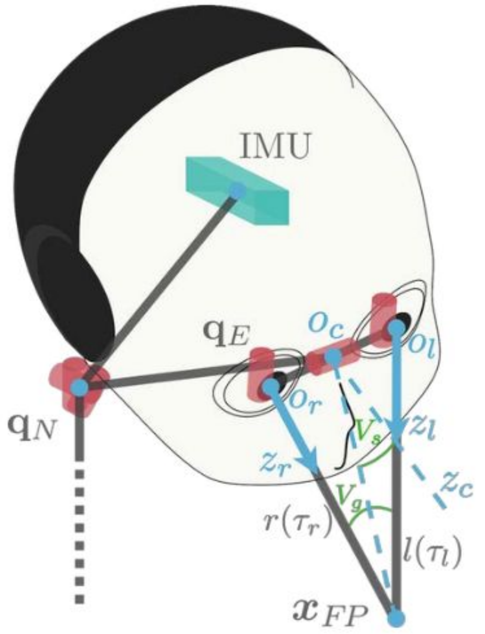

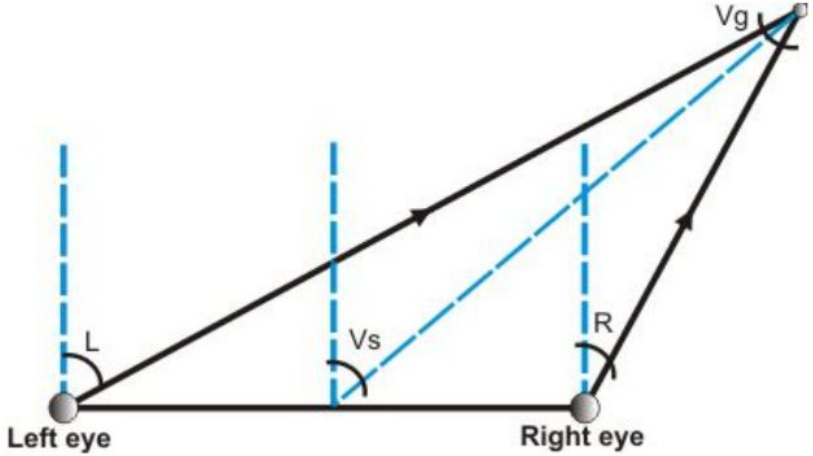

$$\begin{cases} V_g = L - R \\ V_s \approx (L + R)/2 \end{cases}$$

https://github.com/vvv-school/vvv18/blob/master/material/kinematics/kinematics.pdf, courtesy Ugo Pattacini

iCub gaze controller

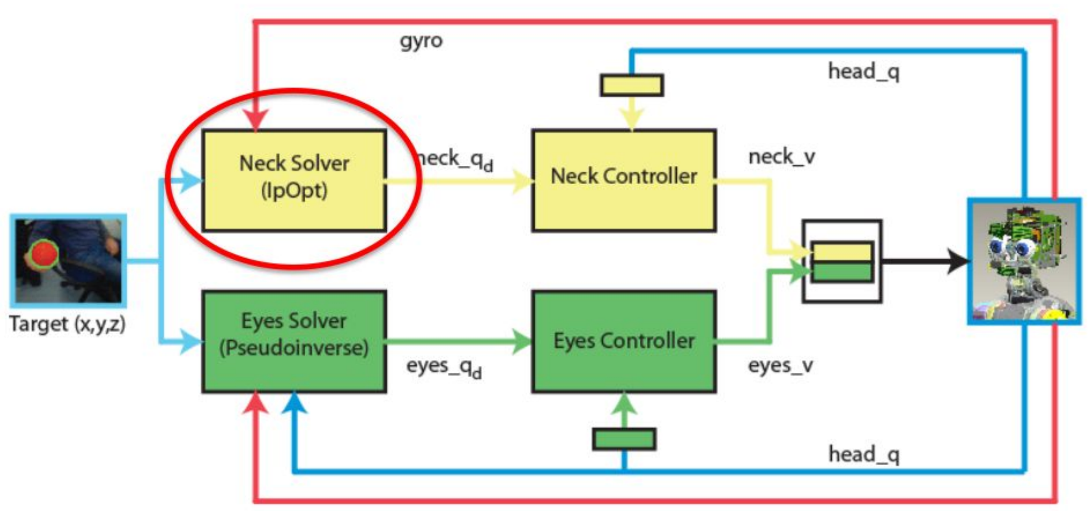

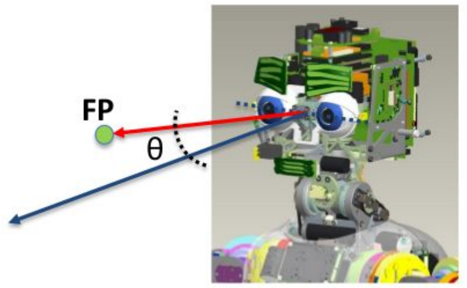

$$q^*_{\text{neck}} = \arg \min_{q_{\text{neck}} \in \mathbb{R}^3} \left\| q_{\text{rest}} - q_{\text{neck}} \right\|^2$$

$$\text{s.t.} \begin{cases} \cos\left(\theta\left(q_{\text{neck}}\right)\right) > 1 - \varepsilon \\ q_{\text{neck}_L} < q_{\text{neck}} < q_{\text{neck}_U} \end{cases}$$

https://github.com/vvv-school/vvv18/blob/master/material/kinematics/kinematics.pdf, courtesy Ugo Pattacini

iCub gaze controller

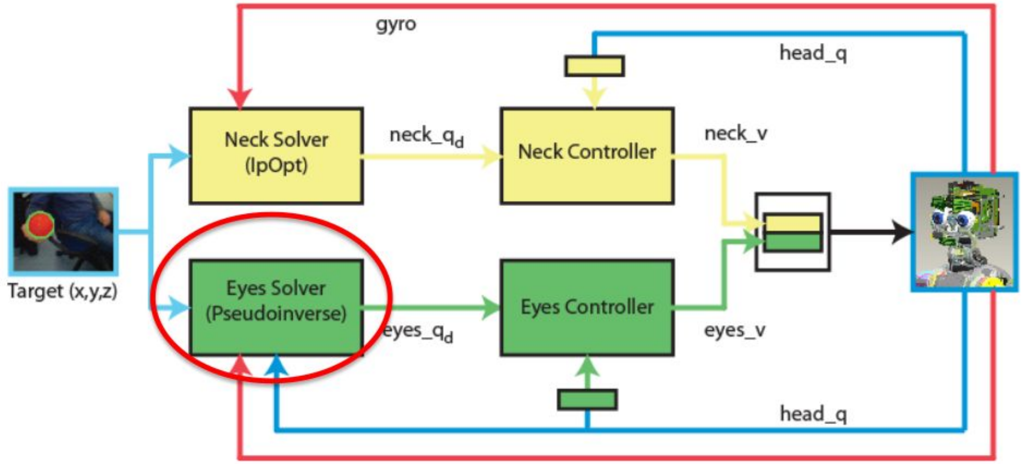

$$q^*_{\text{eyes}} = \arg \min_{q_{\text{eyes}} \in \mathbb{R}^3} \left\| FP_d - K_{FP}\left(q_{\text{eyes}}\right) \right\|^2$$

Gyro

$$q_{\text{eyes}_{t+1}} = q_{\text{eyes}_t} + \Delta T\left(G \cdot J^{\#} \cdot \left(FP_d - K_{FP}\left(q_{\text{eyes}_t}\right)\right) - \boxed{\dot{q}_c}\right)$$

https://github.com/vvv-school/vvv18/blob/master/material/kinematics/kinematics.pdf, courtesy Ugo Pattacini

Inverse kinematics solution under multiple task constraints

- For arm reach of a humanoid, whole-body motion motion may be employed.
- Total number of joints, e.g.: $n_{total} = n_{leg} + n_{torso} + n_{arm} = 6 + 1 + 7 = 17$.
- Degree of kinematic redundancy = 17 - 6 = **11**.
- With such a high degree of redundancy, it is possible to realize multiple additional tasks.

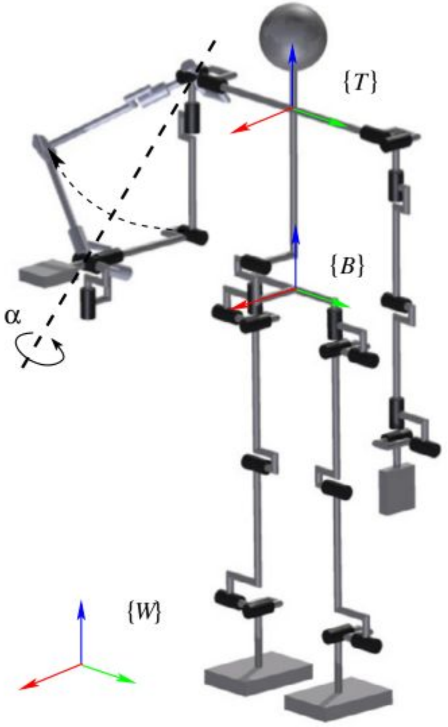

Motion task constraints

- Main task: hand motion ~ reaching.
- Other motion tasks:
  - keep balance
  - avoid obstacles
  - avoid self-collisions
  - avoid singularities
  - avoid joint limits
  - gaze task
  - ...
- Constraints helpful in resolving kinematic redundancy.
  - Caveat: Overconstrained state (task conflict).

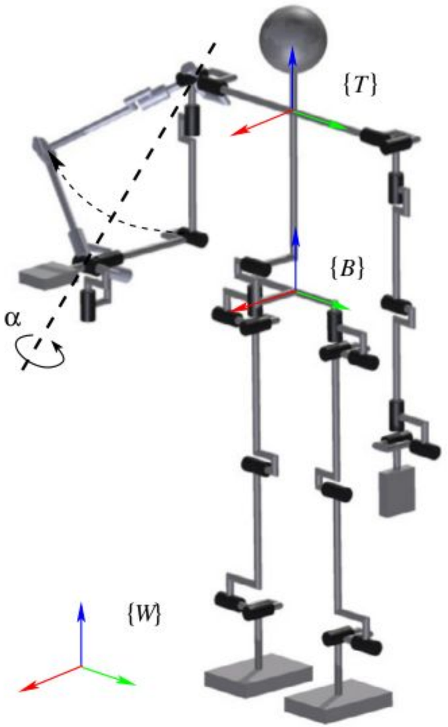

Types of motion task constraints

- link-motion constraints
  - movement of reaching hand
  - movement of Center of Mass
- joint-motion constraints
  - joint ranges
  - joint velocity limits
  - singularity avoidance
- equality- and inequality (unilateral)-type constraints
- permanently active and temporal constraints
- high-priority and low-priority constraints

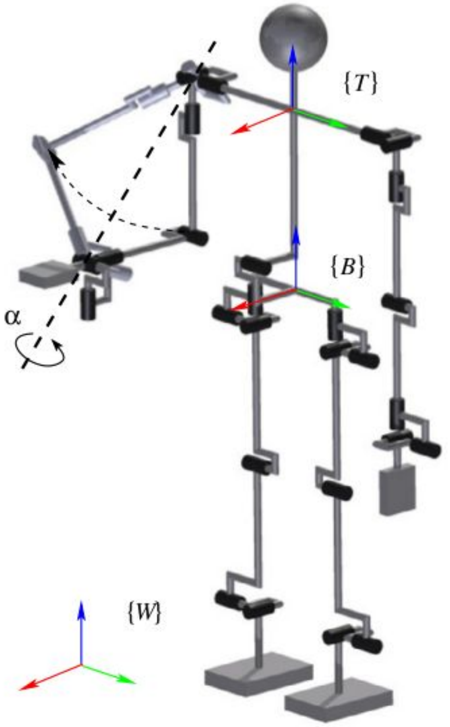

Examples - Classify

- joint limits
  - inequality, permanent, high-priority
- reaching task
  - inequality / minimization term, middle priority
- obstacles
  - inequality, temporal, high priority
- singularities
  - inequality, temporal, middle priority
- postural constraints
  - min. term / inequality, permanent, low-priority

- equality- and inequality (unilateral)-type constraints
- permanently active and temporal constraints
- high-priority and low-priority constraints

Section 2.8.1 in Nenchev, D. N., Konno, A., & Tsujita, T. (2018). Humanoid robots: Modeling and control. Butterworth-Heinemann.

iCub red ball demo - IK solver (+ Cartesian controller) + gaze controller

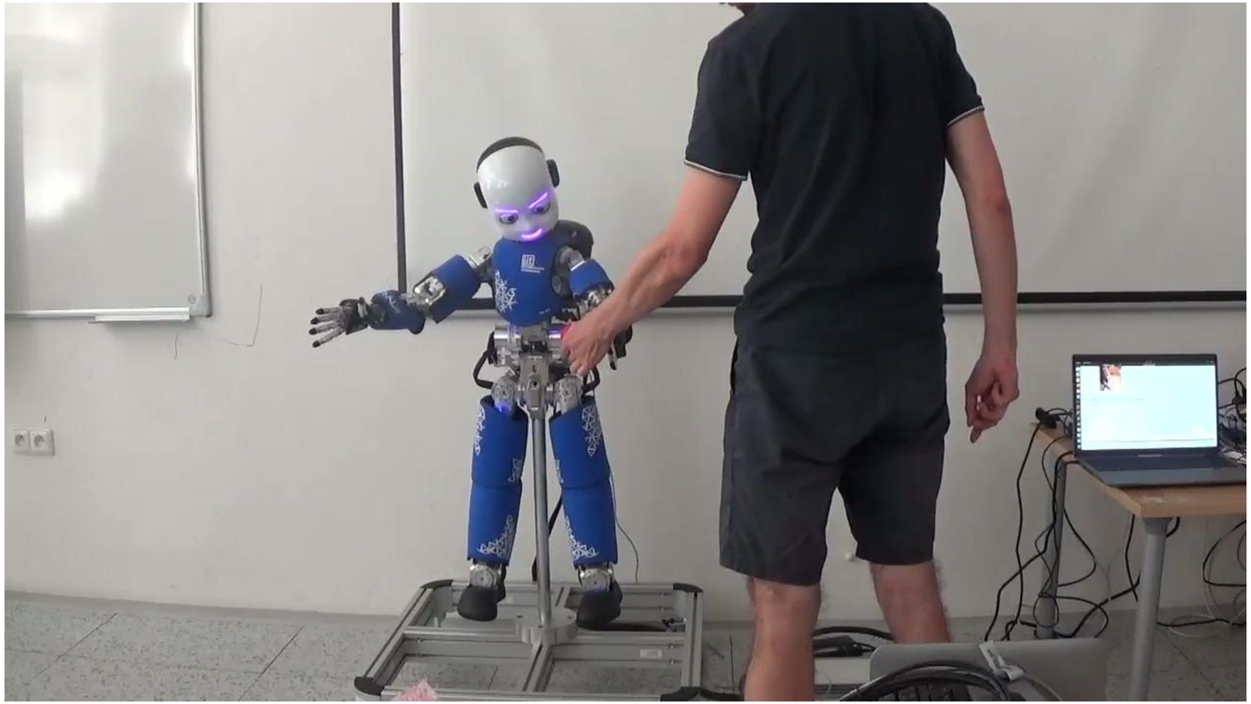

Pattacini, U., Nori, F., Natale, L., Metta, G., & Sandini, G. (2010, October). An experimental evaluation of a novel minimum-jerk Cartesian controller for humanoid robots. In *2010 IEEE/RSJ International Conference on Intelligent Robots and Systems* (pp. 1668-1674). IEEE.

Roncone, A., Pattacini, U., Metta, G., & Natale, L. (2016, June). A Cartesian 6-DoF Gaze Controller for Humanoid Robots. In *Robotics: Science and Systems* (Vol. 2016).

iCub IK solver (+ Cartesian controller) + gaze controller

https://github.com/robotology/icub-basic-demos

- Task 1 - Reach
  - Task DoFs: m = 6
    - https://github.com/robotology/icub-basic-demos/blob/master/demoRedBall/src/main.cpp#L147
  - Joint DoFs: ?
    - m = 7 per arm + 2 of the torso = 9
    - https://github.com/robotology/icub-basic-demos/blob/master/demoRedBall/src/main.cpp#L136
- Task 2 - Gaze
  - Task DoFs: m = 3
  - Joint DoFs: n = 6
  - https://github.com/robotology/icub-basic-demos/blob/master/demoRedBall/src/main.cpp#L898

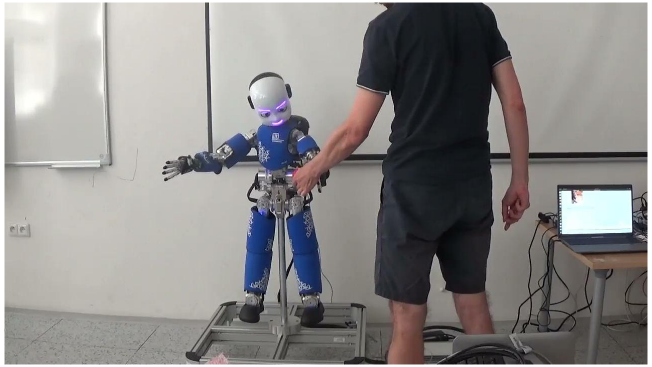

Pattacini, U., Nori, F., Natale, L., Metta, G., & Sandini, G. (2010, October). An experimental evaluation of a novel minimum-jerk Cartesian controller for humanoid robots. In *2010 IEEE/RSJ International Conference on Intelligent Robots and Systems* (pp. 1668-1674). IEEE.

Roncone, A., Pattacini, U., Metta, G., & Natale, L. (2016, June). A Cartesian 6-DoF Gaze Controller for Humanoid Robots. In *Robotics: Science and Systems* (Vol. 2016).

Reactive controller

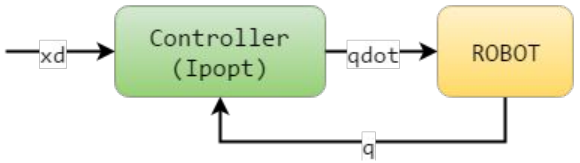

$$\dot{\mathbf{q}}_d = \arg\min_{\dot{\mathbf{q}}\in\mathbb{R}^n}\left(\left\|\bar{\mathbf{x}}_{EEd} - \left(\bar{\mathbf{x}}_{EE} + T_S\mathbf{J}(\bar{\mathbf{q}})\dot{\mathbf{q}}\right)\right\|^2\right)$$

$$\text{s.t.}\begin{cases} \mathbf{q}_L < \bar{\mathbf{q}} + T_S\dot{\mathbf{q}} < \mathbf{q}_U \\ \dot{\mathbf{q}}_L < \dot{\mathbf{q}} < \dot{\mathbf{q}}_U \\ \text{other constraints...} \end{cases}$$

$$\xrightarrow{\textit{obstacles}}$$

$$\begin{cases} \mathbf{s} = -\mathbf{J}_C^T\mathbf{n}_C \cdot V_C \cdot a_{PPS} \\ \dot{q}_{L,i} = \max\{V_{L,i}, s_i\} \quad s_i > 0 \\ \dot{q}_{U,i} = \min\{V_{U,i}, s_i\} \quad s_i < 0 \end{cases}$$

- link-motion constraints
  - movement of reaching hand
  - movement of Center of Mass
- joint-motion constraints
  - joint ranges
  - joint velocity limits
  - singularity avoidance
- equality- and inequality (unilateral)-type constraints
- permanently active and temporal constraints
- high-priority and low-priority constraints

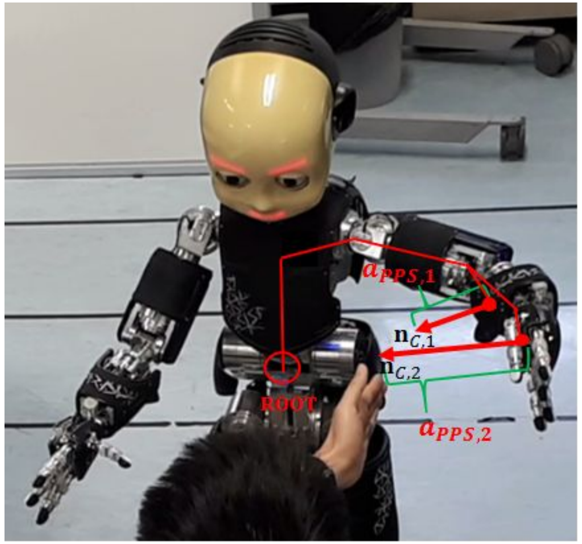

Conflict resolution for multiple motion task constraints

- Inverse kinematics with constraints in a **hierarchical structure**, using null space projections
- How to set priorities? (Sentis & Khatib 2005)
  - joint motion constraints
  - link-motion constraints
    - balance - CoM control
    - hand position
  - postural-variation constraints
- Pros: Stability may be guaranteed.
- Cons: Difficulty of incorporating inequality constraints.

- Inverse kinematics as multiobjective optimization problem
- Pros: All kinds of constraints, incl. inequality constraints, can be incorporated, even on the run.
- Cons: Difficult to guarantee control stability.

Section 2.8.1 in Nenchev, D. N., Konno, A., & Tsujita, T. (2018). Humanoid robots: Modeling and control. Butterworth-Heinemann.
L. Sentis, O. Khatib, Synthesis of whole-body behaviors through hierarchical control of behavioral primitives, International Journal of Humanoid Robotics 02 (2005) 505–518.

iCub Red Ball demo ++

https://youtu.be/NMzhDqVgVvk

Piga, N., Onyshchuk, Y., Pasquale, G., Pattacini, U., and Natale, L., ROFT: Real-time Optical Flow-aided 6D Object Pose and Velocity Tracking, IEEE Robotics & Automation Magazine, vol. 7, no. 1, pp. 159-166, 2022.

iCub balancing and reaching

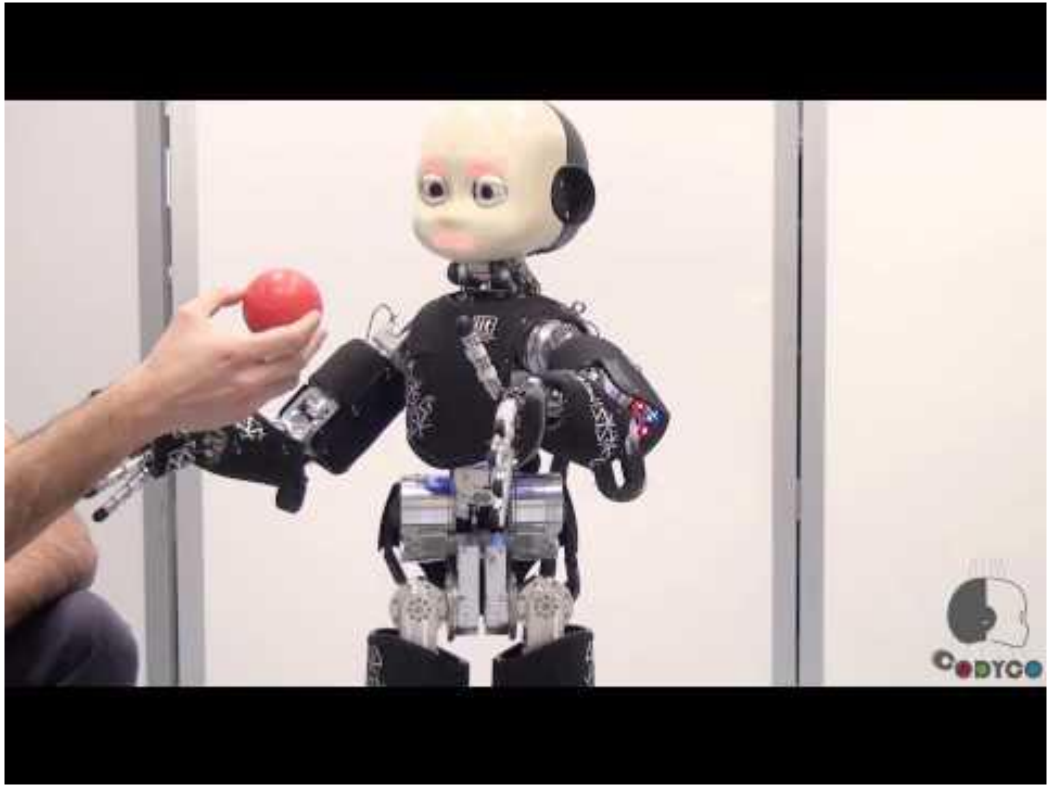

Set of admissible tasks:

- right foot wrench task - regulate the right foot interaction wrench to a predefined value
- left foot wrench
- right arm wrench
- left arm wrench
- postural task
- reaching task
- gaze task

https://youtu.be/7CxaynVnsCI

Nori, F., Traversaro, S., Eljaik, J., Romano, F., Del Prete, A., & Pucci, D. (2015). iCub whole-body control through force regulation on rigid non-coplanar contacts. *Frontiers in Robotics and AI*, 2, 6. https://www.frontiersin.org/articles/10.3389/frobt.2015.00006/full

Resources

- Books
  - Sections 2.4.2 - 2.8 in Nenchev, D. N., Konno, A., & Tsujita, T. (2018). Humanoid robots: Modeling and control. Butterworth-Heinemann.
  - Ch.5 Velocity kinematics and statics in Lynch, K. M., & Park, F. C. (2017). Modern robotics. Cambridge University Press. (see also https://youtu.be/6tj8QLF69Ok)
  - Part III in Corke, P. I. (2013). Robotics, vision and control: fundamental algorithms in MATLAB Berlin: Springer.
- Online resources
  - Howie Choset: https://www.slideserve.com/antonia/inverting-the-jacobian-and-manipulability
  - Modern robotics (Lynch and Park)
    - https://modernrobotics.northwestern.edu/nu-gm-book-resource/velocity-kinematics-and-statics/
  - http://handbookofrobotics.org/view-chapter/videodetails/10
- Articles, book chapters
  - Chiaverini, S., Oriolo, G., & Maciejewski, A. A. (2016). Redundant robots. In *Springer Handbook of Robotics* (pp. 221-242). Springer, Cham.
  - Pattacini, U., Nori, F., Natale, L., Metta, G., & Sandini, G. (2010, October). An experimental evaluation of a novel minimum-jerk cartesian controller for humanoid robots. In *2010 IEEE/RSJ international conference on intelligent robots and systems* (pp. 1668-1674). IEEE.